EFFECTS OF PIRFENIDONE IN A MOUSE LIVER FIBROSIS MODEL

A Thesis

by

OLEKSII SENIUTKIN

Submitted to the Office of Graduate and Professional Studies of
Texas A&M University
in partial fulfillment of the requirements for the degree of

MASTER OF SCIENCE

Chair of Committee,	Ivan Rusyn
Committee Members,	David Threadgill
	Igor Pogribny
Interdisciplinary Faculty Chair,	Ivan Rusyn

May 2017

Major Subject: Toxicology

ABSTRACT

Liver fibrosis results from chronic damage and excessive regeneration with redundant accumulation of extracellular matrix proteins, including collagen. Liver fibrosis may be caused by infectious, environmental, and autoimmune factors. Liver fibrosis is a precursor of cirrhosis and hepatocellular carcinoma. Current treatment options for liver fibrosis are primarily directed at inflammation with few options available to combat fibrogenesis. Pirfenidone (Esbriet®) is an anti-fibrotic agent for treatment of idiopathic pulmonary fibrosis, which downregulates the production of growth factors and procollagens I and II and inhibits fibroblast proliferation. We aimed to test anti-fibrotic potential of pirfenidone in liver using mouse model of sub-chronic cytotoxic fibrosis induced by carbon tetrachloride (CCl_4). Additionally, considering its anti-fibrotic properties, pirfenidone was expected to suppress chemically-induced carcinogenesis.

Several studies were conducted to evaluate effects of pirfenidone in liver. First, a 4-week dose-finding study was performed, male B6C3F1/J mice were treated with CCl_4 (0.2 ml/kg intraperitoneal injections twice a week) while on diet with varying doses of pirfenidone (0 mg/kg, 100 mg/kg, 300 mg/kg, 600 mg/kg). Second, a 14-week subchronic study was conducted, where male B6C3F1/J mice were treated with CCl_4 twice a week while on 300 mg/kg pirfenidone dose diet. Third, a 24-week anti-cancer study was performed, in which 112 male B6C3F1/J mice were exposed to single injection of either N-nitrosodiethylamine

(DEN) or phosphate-buffered saline, followed with 14-week treatment by either olive oil or CCl_4 in combination with either pirfenidone (300 mg/kg) or control diet.

Pirfenidone treatment decreased liver fibrosis in both studies. In dose-finding study, pirfenidone had a significant anti-fibrotic and anti-inflammatory effect by significantly blunting collagen deposition in liver, serum transaminase levels, and preventing ballooning degeneration of hepatocytes at 300 and 600 mg/kg doses. In sub-chronic study, pirfenidone treatment also resulted in a significant reduction in collagen deposition in liver; however, it had little effect on inflammatory markers and liver injury. In anti-cancer study, pirfenidone did not affect incidence, size, or multiplicity of tumors.

Pirfenidone showed anti-fibrogenesis effects in sub-acute and sub-chronic cytotoxic liver fibrosis model; anti-inflammatory effects were observed only in sub-acute study. Pirfenidone has no effect on development of liver tumors in anti-cancer study.

ACKNOWLEDGEMENTS

I am deeply grateful to Dr. Ivan Rusyn for unrelenting support and wise guidance throughout these two years.

I would like to extend my deepest gratitude to members of my Advisory Committee, Dr. David Threadgill (Texas A&M University) and Dr. Igor Pogribny (NCTR).

I would like to sincerely thank Dr. Shinji Furuya, Dr. Joseph Cichocki, Mr. Yu-Syuan Luo and all other members of Dr. Rusyn's Laboratory for their valuable assistance with the experiments and participation in discussions regarding my research project.

I would like to express my sincere gratitude to Dr. Takeki Uehara and Dr. Hiromi Sugimoto (Shionogi & Co., Ltd., Osaka, Japan) for their generous provision of pirfenidone and critical commentaries on course of research, and to Dr. Yuki Kato (Shionogi & Co., Ltd., Osaka, Japan) for performance of histopathological evaluation of tissue samples.

Special acknowledgements are directed towards undergraduate students assisting with animal and laboratory duties.

I owe my deepest gratitude to my family and friends for emotional support and understanding.

CONTRIBUTORS AND FUNDING SOURCES

Contributors

This work was supervised by a Thesis Committee consisting of Professor Ivan Rusyn, advisor and Chair of the Interdisciplinary Faculty of Toxicology in College of Veterinary Medicine and Biomedical Sciences at Texas A&M University, Professor David Threadgill of the Department of Veterinary Pathobiology in College of Veterinary Medicine and Biomedical Sciences at Texas A&M University, and Professor Igor Pogribny of the Division of Biochemical Toxicology at National Center for Toxicological Research (NCTR). The pirfenidone compound used for this research was kindly provided by Shionogi & Co., Ltd. (Osaka, Japan).

All work for the thesis was completed by the student and in active collaboration with Dr. Shinji Furuya and Dr. Joseph Cichocki, postdoctoral fellows of Department of Veterinary Integrative Biosciences in College of Veterinary Medicine and Biomedical Sciences at Texas A&M University. Histopathologic evaluation of tissue slides was performed by Dr. Yuuki Kato of Shionogi & Co., Ltd., Osaka, Japan.

Funding Sources

This work was made possible, in part, by National Institutes of Health under Grant #01AA021908 and by internal funding at Texas A&M University.

Its contents are solely the responsibility of the authors and do not necessarily represent the official views of the National Institutes of Health and Texas A&M University.

NOMENCLATURE

CCl_4 – carbon tetrachloride

DEN - N-nitrosodiethylamine

OO – olive oil

PBS – phosphate-buffered saline

PFD - pirfenidone

CD – control diet

FDA – U.S. Food and Drug Administration

ECM – extracellular matrix

HSC – hepatic stellate cell

PDGF - platelet-derived growth factor

SREBP-1c - sterol regulatory element-binding protein 1c

PPARα - peroxisome proliferator-activated receptor alpha

ROS – reactive oxygen species

HCC – hepatocellular carcinoma

IPF – idiopathic pulmonary fibrosis

TGF-β1 - transforming growth factor beta 1

TNF-α - tumor necrosis factor alpha

ET-1 - endothelin 1

IFN-γ – interferon gamma

SDF-1α - stromal cell-derived factor 1

FGF – fibroblast growth factor

COL1A1 – collagen type I, alpha 1 chain

IL - interleukin

CYP – cytochrome P

MCP-1 - monocyte chemoattractant protein-1

PFD_DS – pirfenidone dose-finding study

PFD_AS – pirfenidone sub-chronic anti-fibrotic study

PFD_MS – pirfenidone anti-cancer study

H&E – hematoxylin and eosin

ALT – alanine aminotransferase

AST – aspartate aminotransferase

CD68 – cluster of differentiation 68

KIM-1 – kidney injury molecule-1

RNA - ribonucleic acid

RT-qPCR – quantitative reverse transcription polymerase chain reaction

IACUC - Institutional Animal Care and Use Committee

TABLE OF CONTENTS

Page

LIST OF FIGURES

Page

Page

LIST OF TABLES

Page

CHAPTER I

INTRODUCTION AND LITERATURE REVIEW

Liver fibrosis: Etiology, pathogenesis, complications, management

Liver fibrosis is a pathologic condition, which develops as a result of repeated, chronic damage, and is characterized by excessive regeneration of parenchyma after progressive destruction, which leads to redundant accumulation of extracellular matrix proteins, including collagen.

Etiologic factors which lead to the development of liver fibrosis are numerous and include various infections (viral – e.g., hepatitis B and hepatitis C viruses; bacterial – e.g., brucellosis; parasitic – e.g., echinococcosis), heavy alcohol consumption with resulting alcoholic liver disease, non-alcoholic fatty liver disease and nonalcoholic steatohepatitis, autoimmune liver diseases (autoimmune hepatitis, primary biliary cholangitis, primary sclerosing cholangitis), certain storage diseases and inborn errors of metabolism (alpha-1 antitrypsin deficiency, Wilson's disease, fructosemia, galactosemia, glycogen storage diseases, hemochromatosis, Gaucher disease, Zellweger syndrome, tyrosinemia), congenital conditions (e.g., congenital hepatic fibrosis) and trauma, as well as multiple medications and toxins [1, 2].

The onset of liver fibrosis is usually asymptomatic. Pathogenesis of hepatic fibrosis constitutes a wound-healing response of the liver to repeated injury, and involves regeneration of parenchymal cells with their replacement of apoptotic and necrotic cells. If hepatic injury persists for a long time, liver regeneration eventually fails, and

hepatocytes are replaced with abundant extracellular matrix (ECM), including collagen. The distribution of ECM is dependent on the type of liver injury, with chronic viral infections and chronic cholestatic conditions resulting in initial deposition of ECM around portal tracts, whereas alcohol-induced liver disease results in deposition of fibrous tissue in pericentral and perisinusoidal regions. There are major differences in ECM composition and quantity (6 times more ECM than normal, including collagens I, III, IV, fibronectin, undulin, elastin, laminin, hualuronan, proteoglycans) in advanced stages of liver fibrosis, compared to normal liver [1, 3].

Hepatic stellate cells (HSCs) are located in the space of Disse, and are main contributors to ECM deposition in the case of liver injury. In case of chronic liver injury, HSCs activate or transdifferentiate into myofibroblast-like cells and obtain contractile, proinflammatory and fibrogenic properties. After activation, HSCs migrate and accumulate at the sites of tissue regeneration and secrete massive amounts of ECM, while also regulating ECM degradation. PDGF, which is primarily produced by Kupffer cells, is the predominant mitogen for activated HSCs [1, 2]. Synthesis of collagen in HSCs is regulated at both transcriptional and posttranscriptional levels. Quiescent HSCs express markers characteristic of adipocytes (SREBP-1c, PPARγ, and leptin), whereas activated HSCs express markers of myogenesis (c-myb, α smooth muscle actin, and myocyte enhancer factor–2). Myofibroblasts derived from small portal vessels also possess potential for fibrogenesis [1, 2].

Relative importance of different cell types in hepatic fibrogenesis is dependent on the origin of liver injury, and complex interactions between various cell types take place.

Injured hepatocytes release ROS and fibrogenic mediators and stimulate the recruitment of white blood cells by inflammatory cells [1].

In the majority of patients, without proper prophylaxis (e. g., avoidance of harmful substances and prompt treatment of chronic viral hepatitis infections) liver fibrosis eventually (usually after 15-20 years) progresses to liver cirrhosis and hepatocellular carcinoma, both of which are severe diseases that constitute a significant segment of morbidity and mortality causes worldwide [1, 3].

Liver cirrhosis is a diffuse pathologic process in liver, which is characterized as an advanced fibrosis with conversion of regular hepatic architecture to structurally aberrant cirrhotic nodules. Progression from hepatic fibrosis to cirrhosis may occur over different amount of years, depending on scale and duration of liver injury [2, 3].

In United States, cirrhosis is the 9th leading cause of death, and holds responsibility for 1.2% of all deaths, with the majority of patients' deaths occurring in their fifth or sixth decades of life. Worldwide, cirrhosis is the 14th most common mortality cause, although in Europe, it is the 4th most common cause of death [2, 3].

Some patients with cirrhosis are asymptomatic and may have relatively normal life expectancy, while other develop a range of symptoms that constitute end-stage liver disease and hold a limited capability of survival. Common signs and symptoms of cirrhosis are derived from decrease in hepatic systemic function (coagulopathy), reduction of hepatic detoxification capacities (hepatic encephalopathy), or chronic increase in venous pressure in portal vein (portal hypertension) [2, 3].

Treatment of cirrhosis is primarily aimed at pharmacologic and procedural management of complications, and bears purely symptomatic relief. Liver transplantation has been evolved as an important strategy in management of decompensated cirrhosis, with quality of life after liver transplant being reported as good or excellent in most cases [2, 3].

Hepatocellular carcinoma (HCC) is a primary malignant tumor of the liver, which, in the majority of cases, occurs in patients with preexisting chronic liver disease and cirrhosis. HCC progress with intrahepatic spread, local expansion, and by metastatic dissemination.

Over the past 20 years, incidence of HCC has grown more than twice, from 2.6 to 5.2 per 100,000 population. The incidence of hepatocellular carcinoma is highest in Asia and Africa, and derives from high prevalence of chronic hepatitis B and C infections, presence of which is a strong predisposition for manifestation of chronic liver disease, which subsequently leads to development of HCC. Hepatocellular carcinoma is currently a third leading cause of cancer-related deaths in the world, and is the fastest growing cause of cancer mortality overall – over the last decade, mortality from HCC increased from 2.8 to 4.7 per 100,000 population [4, 5].

In the past, HCC in most cases presented at advanced stage, with signs and symptoms corresponding to decompensated liver disease, weight loss, and right upper-quadrant pain. At the present time, HCC is primarily recognized at much earlier stage as a consequence of routine screening of individuals with established diagnosis of cirrhosis, utilizing cross-sectional imaging studies and serum alpha-fetoprotein (AFP) measurements [4].

Treatment options for liver fibrosis are scarce and, besides removal of the causative agent as a most effective intervention, primarily consist of suppression of chronic inflammation, which is a major mechanism of the liver fibrosis. Use of anti-inflammatory drugs has been suggested, and corticosteroids are indicated for the treatment of patients with autoimmune hepatitis and acute alcoholic hepatitis. Other experimental treatment strategies include antioxidants (such as vitamin E, silymarin, phosphatidylcholine, and S-adenosyl-L-methionine), inhibitors of signal transduction pathways involved in liver fibrogenesis (pentoxifylline, amiloride, S-farnesylthiosalicylic acid), renin-angiotensin inhibitors, herbal compounds (Sho-saiko-to, glycyrrhizin, Salvia miltiorrhiza), and infusion of mesenchymal stem cells [1, 6].

There is a range of non-organ-specific agents that are proposed to suppress fibrosis development by targeting various mechanisms of fibrosis development, such as TGF-β expression and activation (e.g., pirfenidone), TGF-β signaling pathways (e.g., imatinib, dasatinib), inhibition of fibrocyte homing (e.g., nintedanib, sorafenib), transcription factors (e.g., macrolide antibiotics, rosiglitazone) and other mechanisms (tocilizumab, bosentan, D-penicillamine) [6].

Idiopathic pulmonary fibrosis: Etiology, pathogenesis, management

Idiopathic pulmonary fibrosis is a severe and progressive fibrotic interstitial disease of the lung with an ultimate outcome in form of respiratory failure and death. Median age of establishment of diagnosis is 66 years, and the incidence is increasing with advancement of age.

Currently, no single etiologic agent is established as a common inducement factor in development of IPF. It is currently believed that idiopathic pulmonary fibrosis is an epithelial-fibroblastic disease, in which unestablished environmental or endogenous stimuli disrupt the homeostasis of alveolar epithelial cells, resulting in widespread epithelial cell activation and abnormal epithelial cell repair [7].

Exposure to an induction agent (e. g., smoke, environmental dust, environmental pollutants, viral infections, chronic aspiration, and gastroesophageal reflux disease) in a susceptible person may lead to alveolar epithelial damage, which is followed by aberrant activation of epithelial cells of the alveoli and subsequent migration, proliferation, and activation of mesenchymal cells, which leads to establishment of fibroblastic and myofibroblastic foci. The result of the process described above is excessive accumulation of ECM together with irreversible destruction of lung parenchyma [7].

Upon activation, alveolar epithelial cells release several fibrogenic cytokines and growth factors, including tumor necrosis factor-α (TNF-α), transforming growth factor-β (TGF-β), platelet-derived growth factor, insulin-like growth factor-1, and endothelin-1 (ET-1), all of which are taking part in migration and proliferation of fibroblasts and following transformation of fibroblasts into myofibroblasts (both of which are key cells in fibrogenesis and secretion of ECM proteins). TGF-β showed anti-apoptotic phenotype-promoting properties in fibroblasts. In contrast to normal apoptosis processes that take place in normal wound healing, failure of apoptosis in the event of IPF leads to myofibroblasts accumulation, excessive ECM protein production and pathologic scar formation [7].

There is a number of grave complications that may occur in patients with idiopathic pulmonary fibrosis, including pulmonary hypertension, respiratory infections, acute coronary syndrome, thromboembolic diseases, and lung cancer.

Currently, there are only a few pharmacotherapeutic options for idiopathic pulmonary fibrosis, which can suppress the progression of the disease and improve quality of life for affected patients: *nintedanib*, which is an intracellular inhibitor that targets multiple tyrosine kinases, including CEGF, FGF, and PDGF receptors [8-10], and *pirfenidone*, which is a non-peptide broad-spectrum anti-fibrotic drug that decreases TGF-β1, TNF-α, PDGF and COL1A1 expression [7, 11, 12]. In addition, lung transplantation showed to achieve survival benefit over medical management [7].

Pirfenidone: Overview of anti-fibrotic properties and metabolism

Pirfenidone (5 methyl-1-phenyl-2-(1H)-pyridone; Esbriet®) is an orally bioavailable, synthetic, pyridone compound, which is classified as an immunosuppressant. Pirfenidone is currently the only compound, beside nintedanib, that approved by FDA for the treatment of idiopathic pulmonary fibrosis (IPF) [6]. Existing data from in vitro studies and animal models of pulmonary fibrosis suggest that pirfenidone has antifibrotic, anti-inflammatory and antioxidant properties [11, 12].

Pirfenidone is thought to inhibit progression of fibrosis by affecting tissue levels of various cytokines, growth factors and chemokines. In animal models of pulmonary fibrosis, pirfenidone reduced TGF-β1 production in lungs [11]; in vitro, pirfenidone inhibited TGF-β1-induced differentiation of human lung fibroblasts into myofibroblasts, preventing

excessive collagen synthesis and production of extracellular matrix proteins. In primary alveolar epithelial type II cells and primary lung myofibroblasts isolated from lung parenchyma of patients with IPF, pirfenidone exhibited dose-dependent prevention of pro-proliferative effect of TGF-β1 [11-13]. Pirfenidone is thought to inhibit production of TGF-β1 by preventing reduction of antifibrotic cytokine IFN-γ through suppression of IL-12p40 [6, 11, 12, 14] . Pirfenidone also exhibited suppression of fibroblast proliferation in vitro and reduced elevation of pulmonary levels of IL-18 (lung basic-fibroblast growth factor) and SDF-1α (stroma cell derived factor) in mouse model of pulmonary fibrosis [11].

Anti-inflammatory properties exhibited by pirfenidone were attributed to its regulation of pulmonary inflammatory cytokines and inflammatory cells. Pirfenidone inhibited the release of proinflammatory cytokines such as IL-1β, IL-6, TNF-α, and PDGF (platelet-derived growth factor) in animal models of pulmonary fibrosis [12]. Pirfenidone was noted to suppress IL-1β and TNF-α in alveolar macrophages obtained from bronchoalveolar lavage of patients with IPF [11, 12, 15]. Pirfenidone increased production of IL-10 (anti-inflammatory cytokine) in a murine model of endotoxic shock; in addition, pirfenidone suppressed production of monocyte chemoattractant protein MCP-1 and decreased accumulation of various inflammatory cells, such as lymphocytes, macrophages and neutrophils in hamsters [12, 15]. In pulmonary fibrosis, activation of alveolar macrophages and phagocytosis of neutrophils results in release of ROS, which decreases function of alveolar-capillary beds through lipid peroxidation, resulting in cellular damage [12]. Malonaldehyde, end-product of lipid peroxidation, has been shown to stimulate

collagen synthesis. Pirfenidone scavenged ROS and suppressed lipid peroxidation and malonaldehyde activity in vitro and in animal models of pulmonary fibrosis [12, 15].

Pirfenidone binds mainly to serum albumin in humans, and has an overall mean binding of 50-58% [12]. Pirfenidone was not widely distributed to tissues, with results of a pooled population pharmacokinetic analysis showing an approximate oral steady-state volume of distribution of ~70 L [12]. Pirfenidone is predominantly metabolized by cytochrome P450 pathway. Approximately 70-80% of the compound being metabolized by CYP1A2; CYP2C9, CYP2C19, CYP2D6 and CYP2E1 also take part in metabolism of pirfenidone, albeit to a lesser extent [12]. Mean terminal elimination half-life of pirfenidone after the administration of a single dose of 801 mg in healthy older adults was approximately 2.4 h with food and 2.9 h without food; mean apparent oral clearance of pirfenidone was 13.8 L/h with food and 11.8 L/h without food [12]. Within 24 h of oral administration, approximately 80 % of the pirfenidone dose was excreted in urine. 95% of pirfenidone was excreted as 5-carboxy-pirfenidone (primary metabolite of pirfenidone), with 1% of pirfenidone excreted unchanged and 0.1% excreted as other metabolites [12].

Pirfenidone is expected to suppress development of liver fibrosis and subsequent liver carcinogenesis by targeting same mechanisms of fibrosis as in IPF, and therefore it constitutes an interesting compound that could be used in appropriate experimental liver fibrosis and carcinogenesis model.

Animal models of liver fibrosis and inflammation-associated HCC

Due to genetic and physiologic similarities among rodents and humans, superior breeding capacity and short lifespan, rodents are often used as a study subjects in preclinical research. Experimental animal models constitute an irreplaceable source for clarification of molecular mechanisms of liver fibrosis and development of effective anti-fibrotic therapy strategies.

Current animal models for research of liver fibrosis [16] include:

- *chemically induced fibrosis* using hepatotoxic agents (carbon tetrachloride, thioacetamide, dimethylnitrosamine)
- *cholestatic fibrosis* (bile duct ligation)
- *immunologically mediated fibrosis* (concanavalin A, Schistosoma mansoni infection)

In addition, targeted gene knockouts in mice are evolving as a powerful resource to address the development of mono- and polygenic pathologic conditions by focusing on stable or inducible gene disruption specifically in liver. Considerable amount of data on candidate genes for liver fibrogenesis is currently available resulting from targeted disruption of certain genes, such as IL-6, gp130, gp130/STAT3, SOCS3, SOCS1, Stat5, Bc1-xL, IL-10, fibroblast growth factor receptor 4, 53, adiponectin, TNF-α, CHOP, CD14, leptin, and others [16]. Numerous rodent models have been used to define pathogenesis of hepatocellular carcinoma and have provided a significant contribution to the existing knowledge on HCC.

Current animal models for hepatocellular carcinoma research [17] include:

- *chemically induced models* that are similar to chemically induced liver fibrosis models (administration of DEN, CCl_4, aflatoxin, thiocetamide, peroxisome proliferators and other)
- *xenograft models* (ectopic implantation, orthotopic implantation, hollow fiber model)
- *genetically modified models* (utilizing viral genes, oncogenes and growth factors)

DEN and CCl_4-induced mouse model of fibrosis and inflammation-associated hepatocellular carcinoma [18] was developed by joint efforts of the researchers at University of North Carolina in Chapel Hill, North Carolina, and National Center of Toxicological Research in Jefferson, Arkansas. The disease model is achieved by initial intraperitoneal administration of N-nitrosodiethylamine (DEN) at 8 weeks of age, followed by repeated intraperitoneal administration of carbon tetrachloride (CCl_4) over 14 weeks. A significant potentiation of tumor incidence in liver is observed upon administration of described compounds, resulting in 100% of mice developing liver tumors at 5 months of age [18].

The described model is a reproducible and effective animal study approach that is relatively simple to develop and maintain, and therefore it may be utilized to test anti-fibrotic and anti-cancer efficacy of various compounds in liver, including pirfenidone.

CHAPTER II

SPECIFIC AIMS

Liver fibrosis and its complications in form of liver cirrhosis and hepatocellular carcinoma comprise significant portion of morbidity and mortality in human population, and the best prevention and treatment options are to avoid exposure to a causative agent and in its removal, respectively; however, those strategies are not always achievable [1].

Although many different experimental preventative and therapeutic approaches have been proposed to target progression of liver fibrosis and consequential carcinogenesis, none to this date were found to bear a desirable effect in form of reduction in intensity of liver fibrosis and decrease in incidence of tumorigenesis in livers of experimental animals. Therefore, this project is expected to bring innovation to the field of experimental and clinical hepatology by testing the antifibrotic and anticancer effects of the compound, which has been established as one of the primary treatment options of pulmonary fibrosis [6, 7, 12, 15], but never have been properly tested on hepatic fibrogenesis.

This project is expected to bear a significance in development of new approaches for pharmacologic treatment of liver fibrosis and advanced stage, cirrhosis. Additionally, this project is directed towards targeting hepatic fibrogenesis as a stage of liver cancer development, so there is an expectation of decrease in incidence and multiplicity of liver tumors in experimental animals. Therefore, there is a possibility that acquired results would influence future decisions regarding applications of pirfenidone in human medicine.

Two separate specific aims were established in project to pursue stated goals.

Specific Aim 1: *To test the efficacy of pirfenidone, antifibrotic agent, in reduction of liver fibrosis in mice.*

Rationale: Pirfenidone has proven its efficacy in reducing pulmonary fibrosis through downregulation of the production of growth factors and procollagens I and II. As the mechanisms of fibrosis development are same throughout the organs, pirfenidone is anticipated to affect liver fibrosis as well.

Hypothesis: We hypothesize that pirfenidone would reduce intensity of liver fibrosis in mice.

Approach: To test this hypothesis, we conducted two studies to assess the efficacy of pirfenidone against liver fibrosis. First, we conducted a 4-week study (PFD_DS), in which fibrogenic agent CCl_4 (0.2 ml/kg twice a week) and orally administered pirfenidone in three different doses (100 mg/kg, 300 mg/kg, and 600 mg/kg) were utilized in male mice. Second, we conducted a 14-week study (PFD_AS), in which fibrogenic agent CCl_4 (0.2 ml/kg twice a week) was used along with minimal effective oral dose of pirfenidone (300 mg/kg), which was derived from 4-week study.

Specific Aim 2: *To test the efficacy of pirfenidone, antifibrotic agent, in preventing carcinogenesis in liver.*

Rationale: Liver fibrosis is considered a precursor for the development of liver cancer, specifically hepatocellular carcinoma, in humans. Due to its antifibrotic activity, pirfenidone is expected to suppress fibrogenesis and, subsequently, negatively affect carcinogenesis.

Hypothesis: We hypothesize that pirfenidone would reduce incidence, size and multiplicity of liver tumors in mice.

Approach: To test this hypothesis, we conducted a 24-week initiation-promotion cancer study (PFD_MS), which tests the efficacy of pirfenidone in suppressing development of chemically induced liver tumors. In this study, single intraperitoneal injection of initiation agent DEN and consequent 14-week intraperitoneal administration of promotion agent CCl_4 was utilized along with 14-week dietary application of pirfenidone in minimal effective antifibrotic dose (300 mg/kg), which was established in 4-week study from Specific Aim 1.

CHAPTER III

MATERIALS AND METHODS

Chemicals and diets

DEN (N-nitrosodiethylamine) was obtained from Sigma-Aldrich (St. Louis, MO; CAS 55-18-5). CCl_4 (carbon tetrachloride) was obtained from Sigma-Aldrich (St. Louis, MO; CAS 56-23-5). Olive oil was obtained from Sigma-Aldrich (St. Louis, MO; CAS 8001-25-0). Pirfenidone (5 methyl-1-phenyl-2-(1H)-pyridone) was obtained from Shionogi & Co., LTD (Osaka, Japan; CAS 53179-13-8). Control and pirfenidone-containing grain-based rodent diets were manufactured by Custom Animal Diets, LLC (Easton, PA). BrdU (5-Bromo-2′-deoxyuridine) was obtained from Sigma-Aldrich (St. Louis, MO; CAS 59-14-3). Nembutal was obtained from Oak Pharmaceutical (Lake Forest, IL).

Experimental designs, dosing, and tissue collection

This project consists of three arms, represented in **Figure 1**: *pirfenidone antifibrotic dose-finding study* (PFD_DS), *pirfenidone antifibrotic sub-chronic study* (PFD_AS), and *pirfenidone anti-cancer study* (PFD_MS). PFD_DS targets the effects of different doses of pirfenidone on the reduction of liver fibrosis intensity in mice treated by CCl_4. PFD_AS is an antifibrotic subchronic study that assesses the efficacy of 300 mg/kg dose of pirfenidone, established from PFD_DS, in the event of 14-week CCl_4 administration. PFD_MS is an initiation-promotion liver cancer study that utilizes DEN and CCl_4-induced mouse model of fibrosis and inflammation-associated hepatocellular carcinoma to test the efficacy of pirfenidone in reducing incidence, multiplicity and size of liver tumors.

Figure 1. Combined study design for PFD_DS, PFD_AS, and PFD_MS studies

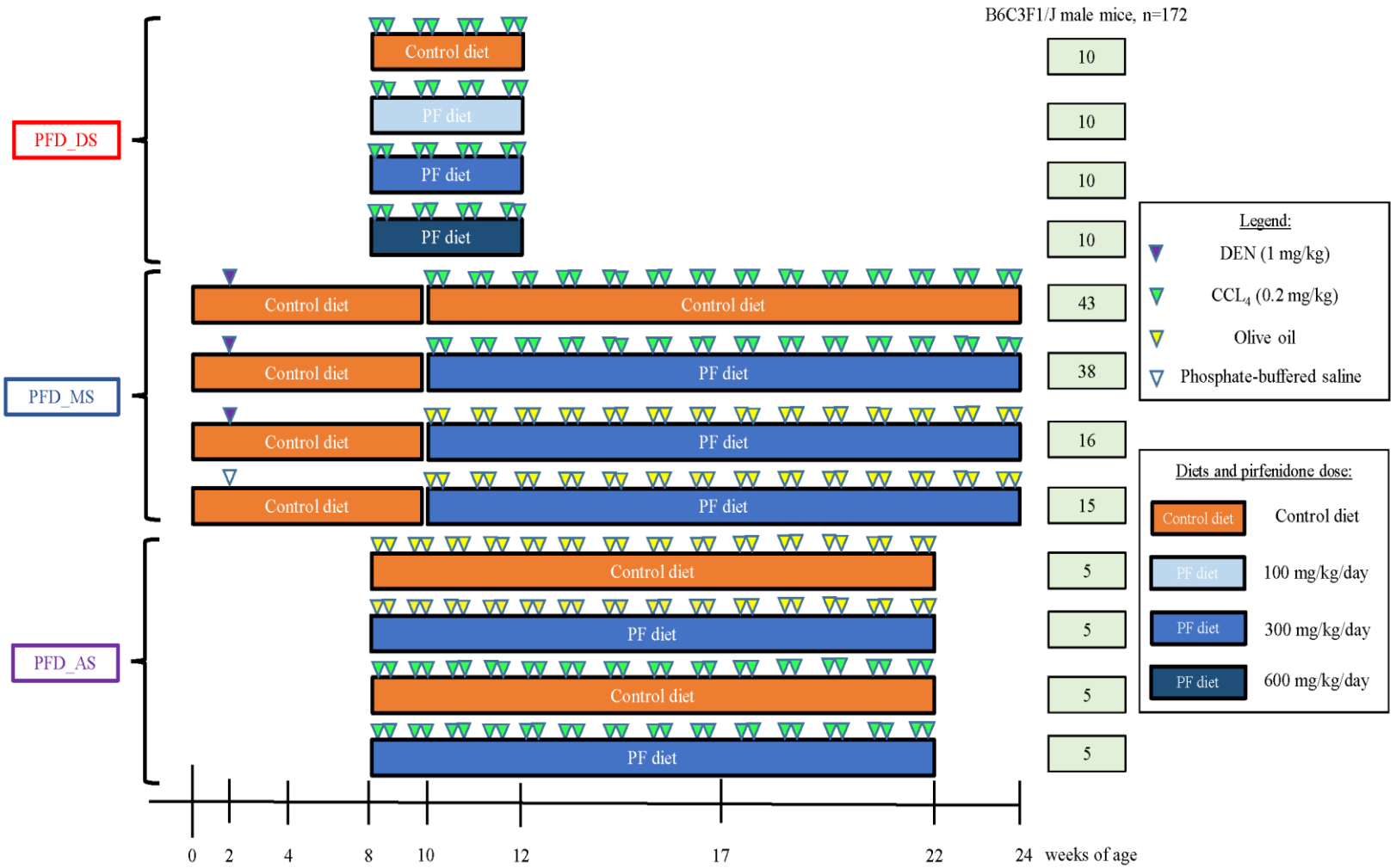

Experimental design of pirfenidone antifibrotic dose-finding study (PFD_DS)

7-week old male B6C3F1/J mice (n=40; The Jackson Laboratory, Bar Harbor, ME) arrived 7 days before the start of experiment and were housed in regular cages in a temperature-controlled (24°C) room, with a 12/12-hr light/dark cycle, and have been granted access to purified water and regular rodent diet *ad libitum*.

After an acclimation period (7 days), the mice were randomly divided into four groups of 10 mice. Beginning at 8 weeks of age, mice from the 1st group started receiving control grain-based rodent diet *ad libitum*. Mice from 2nd, 3rd and 4th groups started receiving custom grain-based rodent diet that contained pirfenidone in concentrations of 0.075% (equivalent to daily oral dose of 100 mg/kg), 0.225% (equivalent to daily oral dose of 300 mg/kg), and 0.45% (equivalent to daily oral dose of 600 mg/kg), respectively. During first 2 weeks of the study, all groups have received their respective diet in powder form due to technical delays with custom pellet diet shipping. Starting from 3rd week, half of mice in each group continued to receive their respective diet in powder form, while other half of animals started to receive pirfenidone diet in pellet form. Mice from each group were injected intraperitoneally with CCl_4 (0.2 ml/kg, diluted in olive oil) twice a week for 4 weeks. Body weight of the animals was assessed twice a week before the injections, and the dosage of CCl_4 was adjusted accordingly to changes in body weight of the animals. During the treatment period, 2 mice from 600 mg/kg group died as a result of possible internal perforation injury, and Unanticipated or Adverse Event Form was submitted to IACUC via iRIS portal.

On the day following last, 8th injection, all animals were euthanized using Nembutal (100 mg/kg intraperitoneal injection) and necropsies were performed. During each necropsy, body weight of animal was recorded, and blood, liver, kidneys, lungs and spleen were collected and weighted. One slice of left liver lobe, one slice of median liver lobe and one slice of kidney from each animal were put inside a plastic cassette and were fixed in 10% neutral buffered formalin for 48 hours. The remaining tissues were immediately frozen in liquid nitrogen and subsequently stored at -80°C for further analysis. All animals were treated humanely and major attention had been paid to alleviation of potential suffering. The experiment was approved by the Institutional Animal Care and Use Committee at Texas A&M University. The experimental design is described in **Figure 2.**

Figure 2. Study design for dose-finding study (PFD_DS)

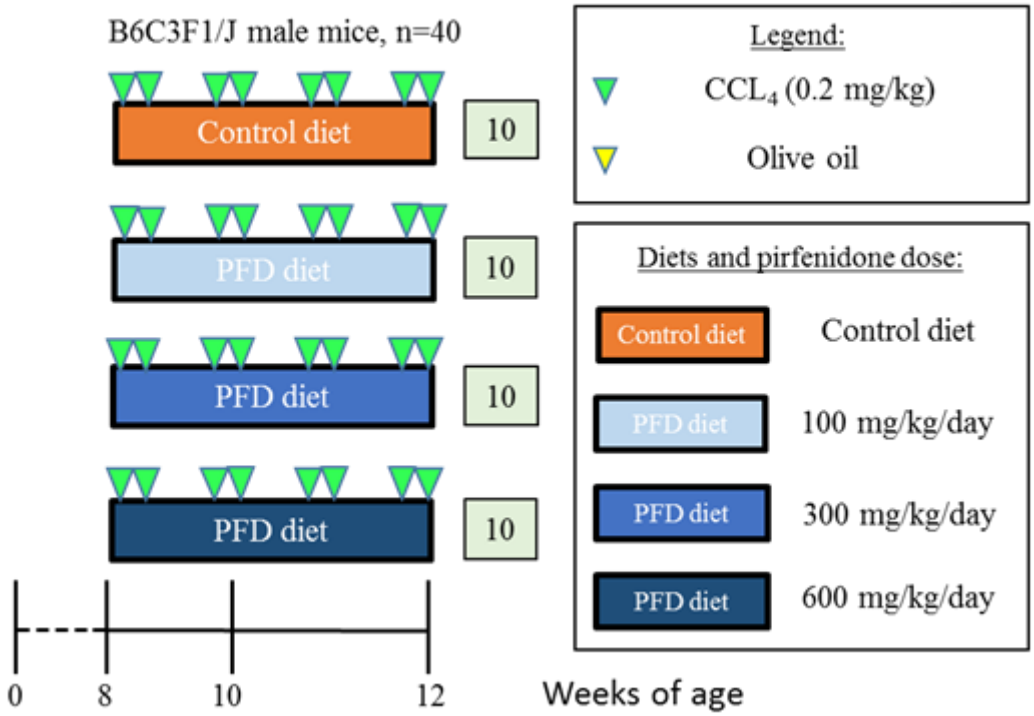

Experimental design of pirfenidone antifibrotic sub-chronic study (PFD_AS)

7-week old male B6C3F1/J mice (n=20; The Jackson Laboratory, Bar Harbor, ME) arrived 7 days before the start of experiment and were housed in regular cages in a temperature-controlled (24°C) room, with a 12/12-hr light/dark cycle, and have been granted access to purified water and regular rodent diet *ad libitum*.

After an acclimation period (7 days), the mice were randomly divided into four groups of 5 mice. Beginning at 8 weeks of age, mice from the 1st and 3rd group started receiving control grain-based rodent diet *ad libitum*. Mice from 2nd and 4th groups started receiving custom grain-based rodent diet that contained pirfenidone in concentration of 0.225% (equivalent to daily oral dose of 300 mg/kg). Mice from 1st and 2nd groups were injected intraperitoneally by olive oil twice a week for 14 weeks, and mice from 3rd and 4th groups were injected intraperitoneally with CCl_4 (0.2 ml/kg, diluted in olive oil) twice a week for 14 weeks. Body weight of the animals was assessed twice a week before the injections, and the dosage of olive oil and CCl_4 was adjusted accordingly to changes in body weight of the animals. During the treatment period, 1 mouse died as a result of possible internal perforation injury.

On the day following last, 28th injection, all animals were euthanized using Nembutal (100 mg/kg intraperitoneal injection) and necropsies were performed. During each necropsy, body weight of animal was recorded, and blood, liver, kidneys, lungs and spleen were collected and weighted. One slice of left liver lobe, one slice of median liver lobe and one slice of kidney from each animal were put inside a plastic cassette and were fixed in 10%

neutral buffered formalin for 48 hours. The remaining tissues were immediately frozen in liquid nitrogen and subsequently stored at -80°C for further analysis. All animals were treated humanely and major attention had been paid to alleviation of potential suffering. The experiment was approved by the Institutional Animal Care and Use Committee at Texas A&M University. The experimental design for this study is described in **Figure 3.**

Figure 3. Study design for sub-chronic study (PFD_AS)

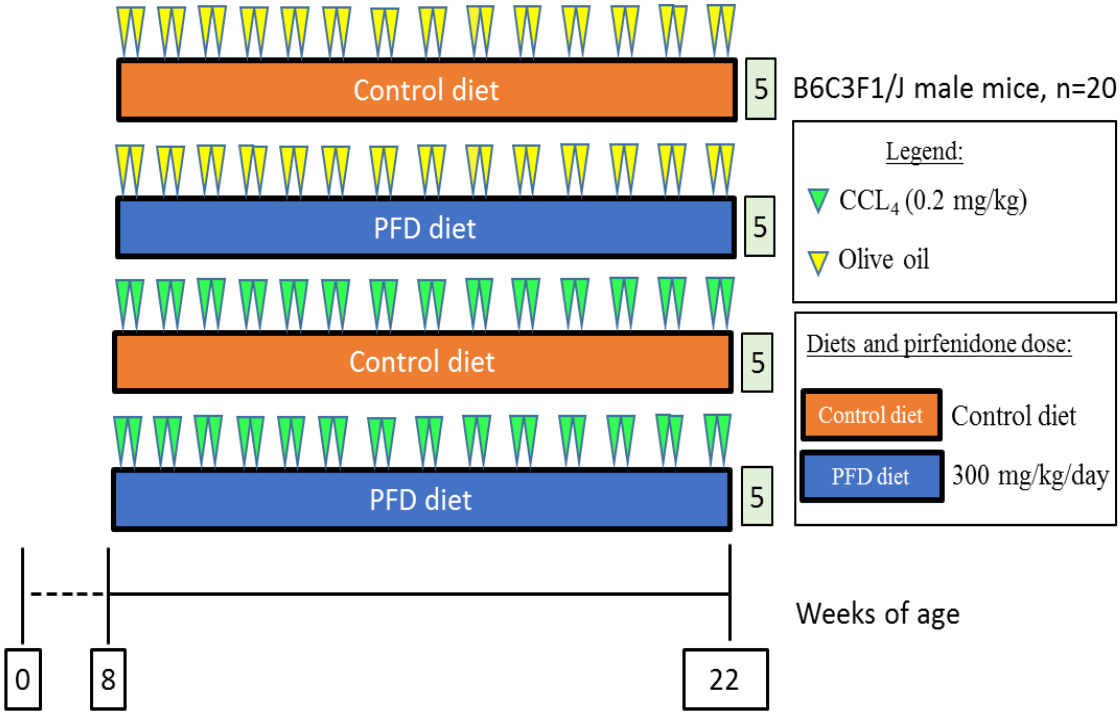

Experimental design of pirfenidone anti-cancer study (PFD_MS)

1-week old male B6C3F1/J mice (n=112; The Jackson Laboratory, Bar Harbor, ME) arrived 7 days before the start of experiment together with AXEAST: AX27 and AXEAST: AX28 female mice acting as foster mothers, with a maximum of 5 pups per 1 foster mother (n=23; The Jackson Laboratory, Bar Harbor, ME). All mice were housed in regular cages in a temperature-controlled (24°C) room, with a 12/12-hr light/dark cycle, were granted access to purified water and regular rodent diet *ad libitum*, and were left intact for an acclimation period, which lasted 7 days. On 14th day after birth, the pups were randomly divided into two groups – 1st group of pups (n=97) receiving DEN (1 mg/kg, dissolved in phosphate-buffered saline, single intraperitoneal injection) and 2nd group of pups (n=15) receiving sterile phosphate-buffered saline (1 mg/kg, single intraperitoneal injection). At 10 weeks of age, all mice were split into four groups for the purpose of receiving appropriate diets *(ad libitum)* and corresponding chemical injections (twice weekly). Mice from the 1st group began receiving control diet. Mice from the 2nd, 3rd and 4th groups began receiving diet containing 0.225% pirfenidone, equivalent to daily oral dose of 300 mg/kg. Starting from 10 weeks of age, mice from groups 1 and 2 were injected intraperitoneally with CCl_4 (0.2 ml/kg, diluted in olive oil) and mice from groups 3 and 4 were injected intraperitoneally by olive oil alone twice a week for 14 weeks. Body weight of the animals was assessed twice a week before the injections, and the dosage of CCl_4 and olive oil was adjusted accordingly. During the treatment period, 1 mouse from DEN+CCl_4/CD group died as a result of possible internal perforation injury, and Unanticipated or Adverse Event Form was submitted to IACUC via iRIS portal. On the

day following last, 28th injection, all animals were euthanized using Nembutal (100 mg/kg intraperitoneal injection) and necropsies were performed. During each necropsy, body weight of animal was recorded, and blood, liver, kidneys, lungs and spleen were collected and weighted. Macroscopic evaluation and quantification of visible liver tissue tumors was performed. One slice of left liver lobe, one slice of median liver lobe, one slice of kidney, and a segment of duodenum from each animal were put inside a plastic cassette and were fixed in 10% neutral buffered formalin for 48 hours. The remaining tissues were immediately frozen in liquid nitrogen and stored at -80°C for further analysis. All animals were treated humanely and major attention had been paid to alleviation of potential suffering. The experiment was approved by the Institutional Animal Care and Use Committee. Experimental design of this study is shown in **Figure 4.**

Figure 4. Study design for anti-cancer study (PFD_MS)

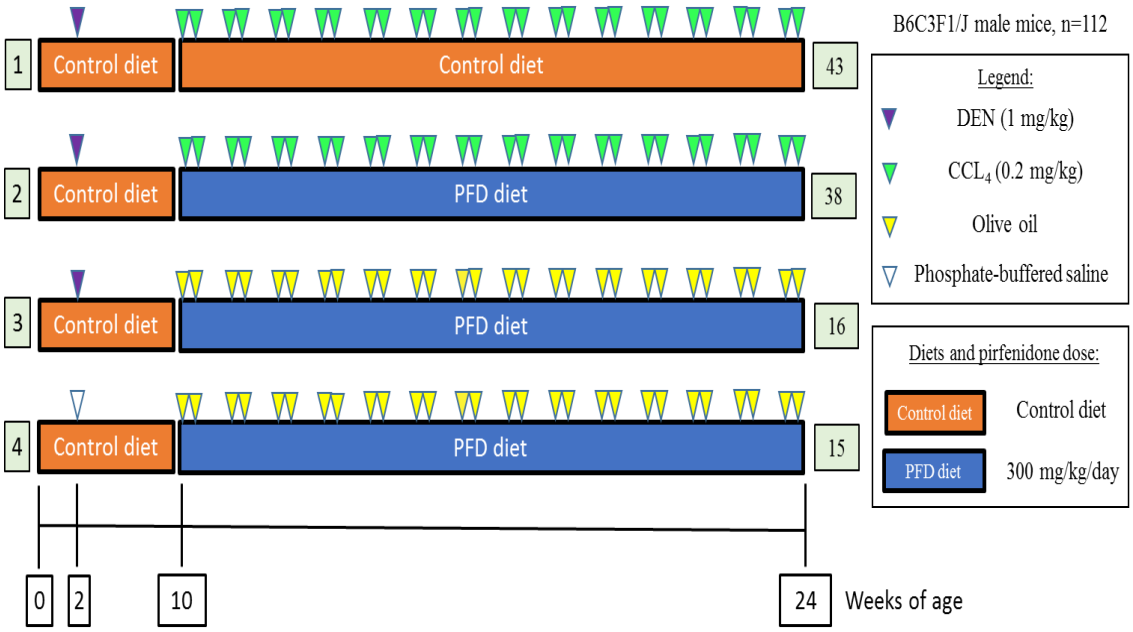

Histopathological evaluation of liver tissue

Tissues were embedded in paraffin, sectioned at 5 µm, and hematoxylin and eosin (H&E) and Sirius Red staining techniques of liver tissue were performed according to standard protocols.

For H&E staining, samples were evaluated in a blind manner by a certified veterinary pathologist, and total histopathological score was established using the parameters of *peripheral* and *focal necrosis, peripheral ballooning cells, inflammatory infiltration,* and *peripheral fibrosis.* Ballooning degeneration is an often-used term in liver morphology, which indicates hepatocyte degeneration that is associated with swelling, rounding, and enlargement of hepatocytes, along with characteristically reticulated cytoplasm [19]. Application of this term has been observed in acute viral hepatitis, alcoholic and non-alcoholic steatohepatitis, autoimmune hepatitis, Wilson's disease, neonatal giant cell hepatitis, toxic liver damage and ischemia/reperfusion injury of liver allografts cases. Shape and size of hepatocytes may be affected by the amount of intracellular organelles and other cytoplasmic components, cytoskeletal architecture, fluid retention, or a combination of these factors [19]. The following histopathological scoring system was utilized: 0 - No Change; 1 - Very slight change; 2 - Slight change; 3 - Moderate change; 4 – Severe change.

Sirius Red (Direct Red 80) is a polyazo dye, which is used in a diversity of clinical cases with the primary objective of observing extent of fibrosis in the event of inflammation caused by developing cancer, vascular, or metabolic pathologies. Using bright field

microscopy, nuclei and cytoplasm of cells could be seen in yellow color, while collagen fibers gain varying shades of red color. For Sirius Red staining, quantitative analysis was performed using ImageJ (https://imagej.nih.gov/ij/) at x100 magnification in four fields of liver tissue, which were randomly selected to calculate percent of positively stained area.

Immunohistochemistry

For CD68 antibody staining of liver tissue, paraffin-embedded liver sections (5 μm thick) were stained with primary antibodies using Dako Antibody Dilution solution (Dako, Carpinteria, CA). The primary antibody used in this experiment was rat anti-mouse CD68 (MCA1957GA; Bio-Rad, Raleigh, NC; 1:50, 1 hour, room temperature). ABC method was performed by using VECTASTAIN Elite ABC HRP Peroxidase Rat IgG Kit (PK-6104; Vector Laboratories, Burlingame, CA). Dako Liquid DAB+ Substrate chromogen System (Dako, Carpinteria, CA) was employed for visualization. Slides were counterstained with filtered Mayer's hematoxylin (Sigma) for 60 seconds. Quantitative analysis was performed manually by counting CD68-positive cells at x200 magnification in four fields of liver tissue, which were randomly selected to calculate percent of positively stained area.

KIM-1 staining of kidney tissue specifically marks Kidney Injury Molecule-1 (KIM-1), type 1 transmembrane protein, expression of which is markedly upregulated in proximal kidney tubule in the event of acute kidney injury [20]. For KIM-1 antibody staining of kidney tissue, paraffin-embedded kidney sections (5 μm thick) were stained with primary antibodies using Dako Antibody Dilution solution (Dako, Carpinteria, CA). The primary

antibody used in this experiment was: goat anti-mouse KIM-1 (AF1817; R&D Systems, Minneapolis, MN; 1:50, 1 hour, room temperature). Rabbit anti-goat IgG Antibody, HRP conjugate (AP106P; EMD Millipore, Billerica, MA, 1:2000, 1 hour, room temperature) was used secondarily. Dako Liquid DAB+ Substrate chromogen System (Dako, Carpinteria, CA) was employed for visualization. Slides were counterstained with filtered Mayer's hematoxylin (Sigma) for 60 seconds. Quantitative analysis was performed manually by counting number of KIM-1 positive proximal tubules and calculating ratio of CD68-positive cells at x200 magnification in four fields of kidney tissue, which were randomly selected to calculate percentage of positively stained area.

Serum clinical chemistry

Hepatocellular damage releases transaminase enzymes, specifically alanine aminotransferase (ALT) and aspartate aminotransferase (AST), into the bloodstream. ALT is primarily contained in the liver; however, AST is also found in erythrocytes and skeletal muscle [21]. Therefore, serum ALT elevations are, generally speaking, more specific for hepatic injury [21].

Serum collection was performed at the time of necropsies via Z-gel tubes (Sarstedt, Nümbrecht, Germany). Serum alanine aminotransferase (ALT) and serum aspartate aminotransferase (AST) levels were measured with a commercially-available kit (Sigma Aldrich, St. Louis, MO) according to manufacturer's instructions.

RNA isolation and quantitative reverse transcription PCR

Total RNA was extracted from liver using the RNeasy Mini kit (Qiagen, Valencia, CA). RNA concentrations were measured with NanoDrop ND-1000 spectrophotometer (NanoDrop Technologies, Wilmington, DE) and quality was verified using the Bio-Analyzer (Agilent Technologies, Santa Clara, CA).

Total RNA was reverse transcribed using random primers and the high capacity cDNA archive kit (Applied Biosystems, Foster City, CA). Reactions were performed in a 96-well assay format using a QuantStudio™ 7 Flex Real-Time PCR System (Life Technologies). The mRNA level of the housekeeping gene, TATA-Box binding protein (Tbp; Hs00427620_m1), was evaluated in tandem with each experimental run. The relative level of each transcript was determined using the 2-ΔΔCt method [22].

Primers, which were used for detection of gene expression of pro-inflammatory markers, CYP450 superfamily enzymes, and kidney injury markers, are shown in **Table 1.**

Table 1. List of primers used in RT-qPCR for detection of gene expression of pro-inflammatory markers, CYP450 enzymes, and kidney injury markers

Gene Name	**Gene Symbol**	**Assay ID**	**Organ**
Tumor necrosis factor alpha	*Tnf*	Mm00443258_m1	Liver
TIMP metallopeptidase inhibitor 1	*Timp1*	Hs01092512_g1	
Interleukin 1 beta	*Il1*	Hs01555410_m1	
Transforming growth factor beta 1	*Tgfb1*	Hs00998133_m1	
C-C motif chemokine receptor 5	*Ccr5*	Hs99999149_s1	
NAD(P)H quinone dehydrogenase 1	*Nqo1*	Hs01045993_g1	
Heme oxygenase 1	*Hmox1*	Hs01110250_m1	
Epithelial cell adhesion molecule	*Epcam*	Hs00901885_m1	
CD68 molecule	*Cd68*	Hs02836816_g1	
Alpha fetoprotein	*Afp*	Hs01040598_m1	
Keratin 7	*Krt7*	Hs00559840_m1	
Cytochrome P450 1 A 2	*Cyp1a2*	Hs00167927_m1	Liver, kidney
Cytochrome P450 2 B 10	*Cyp2b10*	Mm01972453_s1	
Cytochrome P450 2 E 1	*Cyp2e1*	Hs00559367_m1	
Cytochrome P450 3 A 11	*Cyp3a11*	Mm00731567_m1	
Cytochrome P450 4 A 10	*Cyp4a10*	Mm02601690_gH	
Hepatitis A virus cellular receptor 1	*Kim1*	Hs00930379_g1	Kidney

Western blot analysis of CYP2E1

Liver tissue lysates were prepared by homogenization in lysis buffer (50mM Tris-HCl, pH 7.4; 1% NP-40; 1.0% sodium dodecyl sulfate; 150mM NaCl; 1mM EDTA; 1mM PMSF; and 1.5mM dithiothreitol), sonication, and incubation at 4°C for 30 min, followed by centrifugation at 10,000 g at 4°C for 10 min. Protein concentrations in the extracts were quantified by Bradford assay (Bio-Rad, Hercules, CA) using Synergy™ H4 hybrid multi-mode microplate reader (BioTek, Winooski, VT). Extracts containing equal quantities of proteins were separated by SDS-PAGE on 15% polyacrylamide gels and transferred to PVDF membranes. Membranes were probed with primary antibody against cytochrome P450 2E1 protein (ab28146; Abcam, Cambridge, MA; 1:1000). Blots were scanned and analyzed using the Odyssey CLx Infrared Imaging System (LI-COR Biosciences). Amido Black staining of proteins on transferred membrane blots was performed.

Statistical analysis

Statistical significance was determined using GraphPad Prism5 v5.0 (San Diego, CA). Quantitative values are expressed as mean±SD unless otherwise noted. Statistical significance was evaluated using one-way ANOVA within each time point followed by the Tukey's post hoc test. Statistical significance is indicated at any level below $p < 0.05$.

CHAPTER IV

RESULTS

Results of dose-finding study (PFD_DS)

PFD_DS is a 4-week dose-finding study, in which 40 male B6C3F1/J mice were treated with CCl_4 (0.2 ml/kg intraperitoneal injections twice a week) while on diet with varying doses of pirfenidone (0 mg/kg, 100 mg/kg, 300 mg/kg, 600 mg/kg). Experimental design for this study is described in **Figure 2.**

Body and organ weight

Body weight was measured regularly to track the general state of health of animals. Animals in every group were gaining body weight over the duration of the study; mice in CCl_4+300 mg/kg pirfenidone diet and CCl_4+600 mg/kg pirfenidone diet groups have shown to gain weight more slowly, as compared to CCl_4+CD and CCl_4+100 mg/kg pirfenidone diet group **(Figure 5).** A noticeable 6-8% drop in body weight was observed among the groups after several initial intraperitoneal injections of either olive oil or carbon tetrachloride. This negative change may be explained by overall stress of animals and change in eating habits after the initiation of intraperitoneal injections containing irritative compounds. This decrease in body weight did not affect the course of the study. After all mice adjusted to the procedure and new diet, their weight started to increase on day 6 of injections. Subsequently, several minor fluctuations in body weight among all treatment groups were observed on days 10 and 26, which did not affect the course of the study.

Figure 5. Body weight change among treatment groups (A) and further stratification of groups by different diet forms (B) in dose-finding study (PFD_DS)

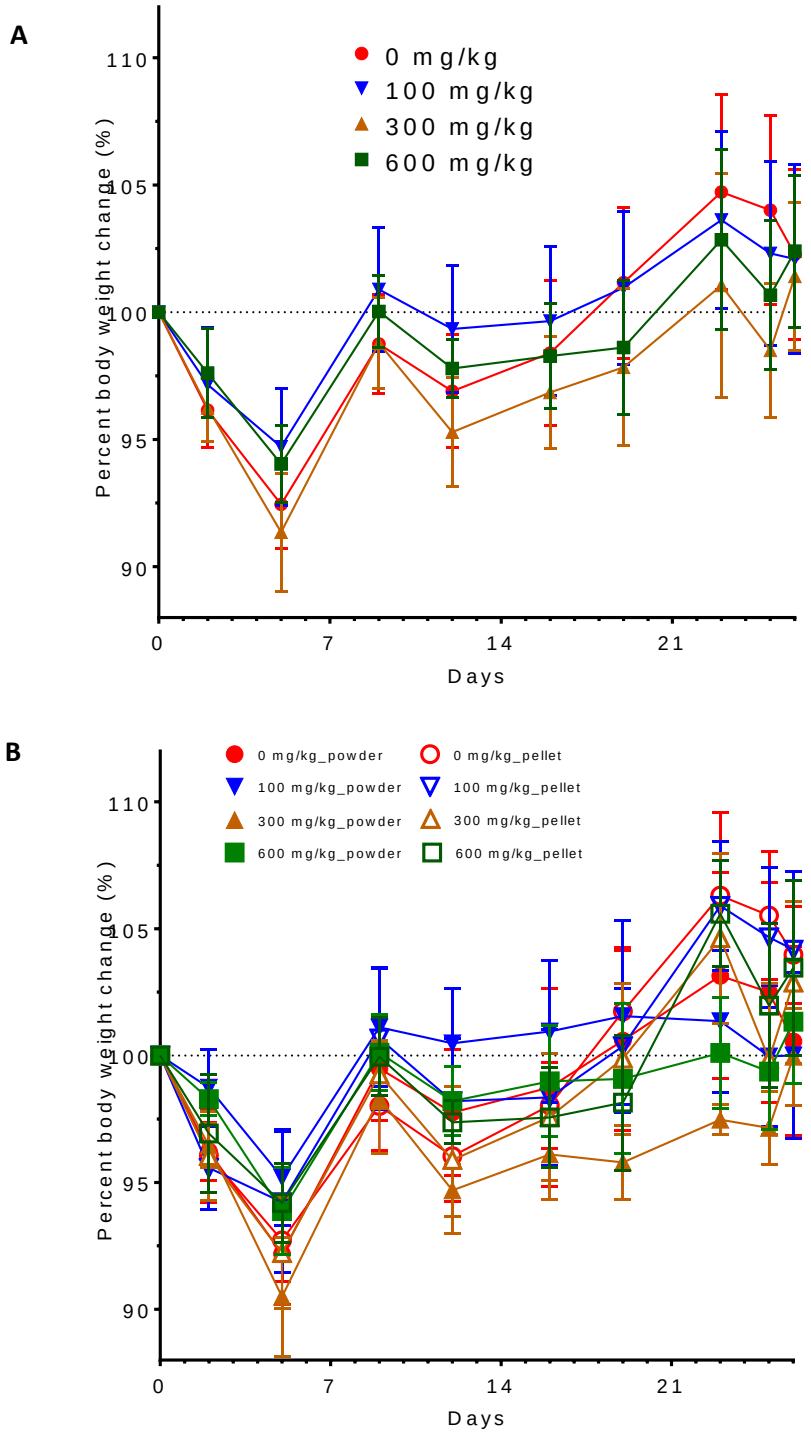

Relative liver weight was significantly increased in CCl_4+300 mg/kg pirfenidone diet compared to CCl_4+CD group. Relative liver weight was also increased in CCl_4+600 mg/kg pirfenidone diet group compared to both CCl_4+CD and CCl_4+100 mg/kg pirfenidone diet groups **(Figure 6).** There was no significant difference in relative kidney weight, relative spleen weight, and relative lung weight among the treatment groups **(Figure 6).**

Figure 6. Relative liver (A), kidney (B), spleen (C), and lung (D) weights in dose-finding study (PFD_DS). All data are presented as mean ± SD. [a]$p < 0.05$, compared to CCl_4+CD group; [b]$p < 0.05$, compared to CCl_4+PFD(100mg/kg) group; NS describes no significant difference among groups

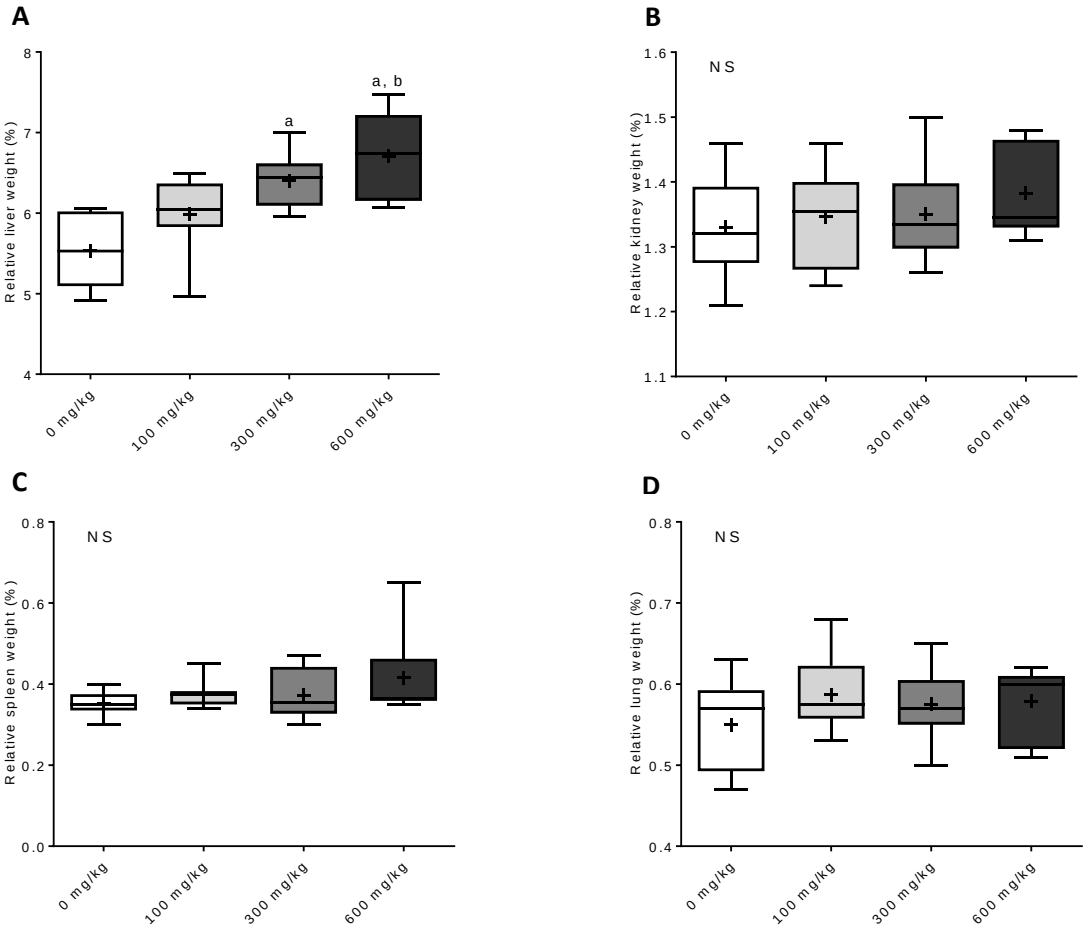

Serum clinical chemistry

Alanine aminotransferase (ALT) and aspartate aminotransferase (AST) serum levels were significantly decreased and AST to ALT ratio was significantly higher in CCl_4+300 mg/kg pirfenidone diet and CCl_4+600 mg/kg pirfenidone diet groups, compared to CCl_4+CD group, with no significant difference between diets in pellet and powder forms **(Figure 7).**

Figure 7. Serum ALT and AST in dose-finding study (PFD_DS). All data are presented as mean ± SD.
Top row: $^{a}p < 0.05$, compared to CCl_4+CD group; $^{b}p < 0.05$, compared to CCl_4+PFD (100mg/kg) group; $^{c}p < 0.05$, compared to CCl_4+PFD (300mg/kg) group; $^{d}p < 0.05$, compared to CCl_4+PFD (600mg/kg). *Bottom row*: $^{a}p < 0.05$, compared to CCl_4+CD (powder form) group; $^{b}p < 0.05$, compared to CCl_4+CD (pellet form) group; $^{c}p < 0.05$, compared to CCl_4+PFD (100mg/kg, powder form) group; $^{d}p < 0.05$, compared to CCl_4+PFD (100mg/kg, pellet form)

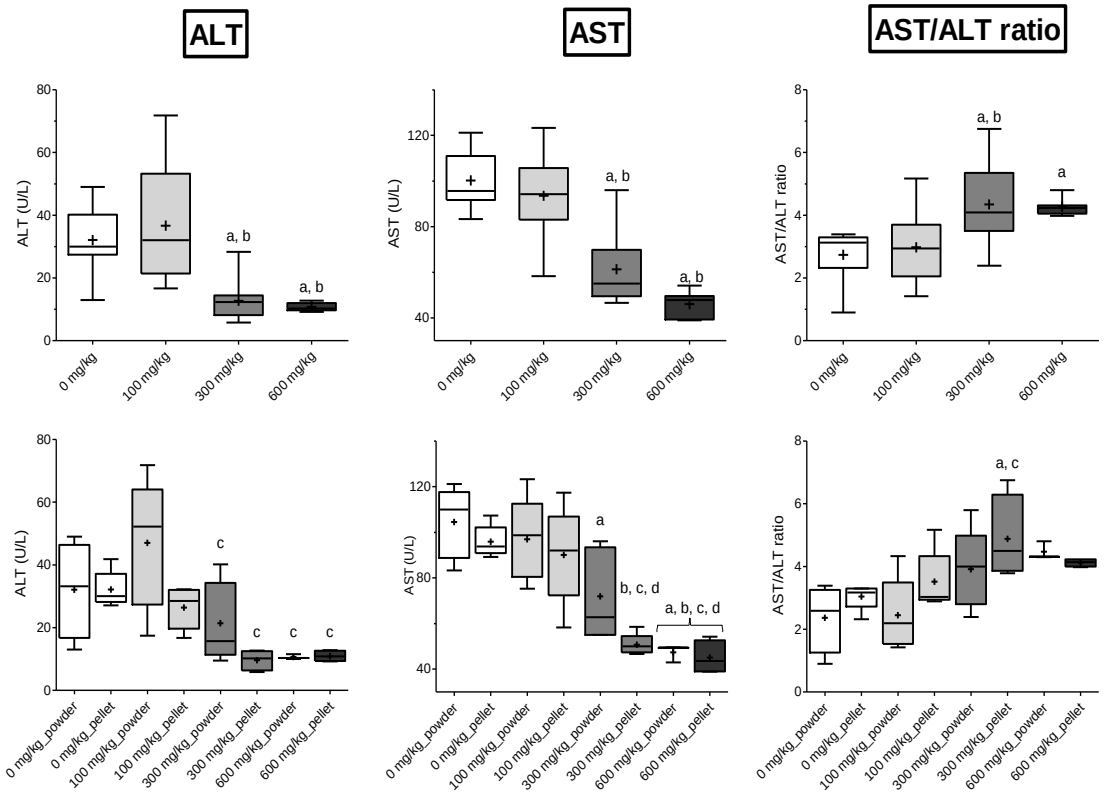

Histopathological evaluation of liver tissue

Hematoxylin and eosin staining of liver tissue slides was performed. Hepatocellular necrosis (arrow), cellular infiltration (inflammation), and ballooning cell accumulation (hydropic degeneration, arrowhead) were observed in the centrilobular region of liver among all treatment groups, with a visible decrease in intensity of all described parameters correlating with an increase in dosage of pirfenidone (representative image of H&E staining of mouse liver from CCl_4+CD treatment group is shown in **Figure 8**).

Figure 8. Representative histology of CCl_4/CD-treated, H&E-stained mouse liver in dose-finding study (PFD_DS). Hepatocellular necrosis is shown by *arrow* and ballooning cell accumulation (hydropic degeneration) is shown by *arrowhead*. Original magnification is x200

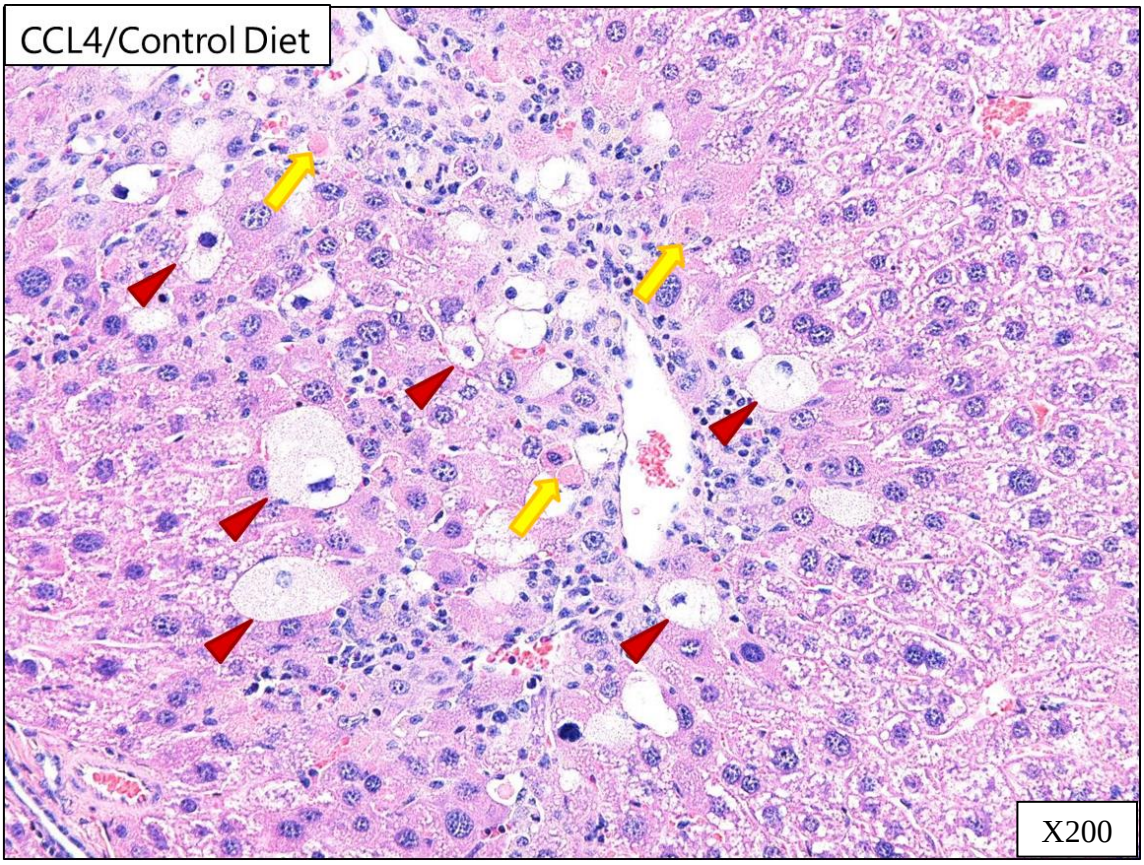

Total histopathology score was calculated, using the parameters of *necrosis, ballooning, inflammation,* and *fibrosis* **(Figure 9).** Both CCl_4+300 mg/kg pirfenidone diet and CCl_4+600 mg/kg pirfenidone diet groups have shown significantly lower histopathology score values in comparison to CCl_4+CD group.

Figure 9. Total histopathology score (A) in dose-finding study (PFD_DS). Four parameters were used to calculate total score (B).
All data are presented as mean ± SD. [a]$p < 0.05$, compared to CCl_4+CD group; [b]$p < 0.05$, compared to CCl_4+PFD (100mg/kg) group; NS describes no significant difference among groups

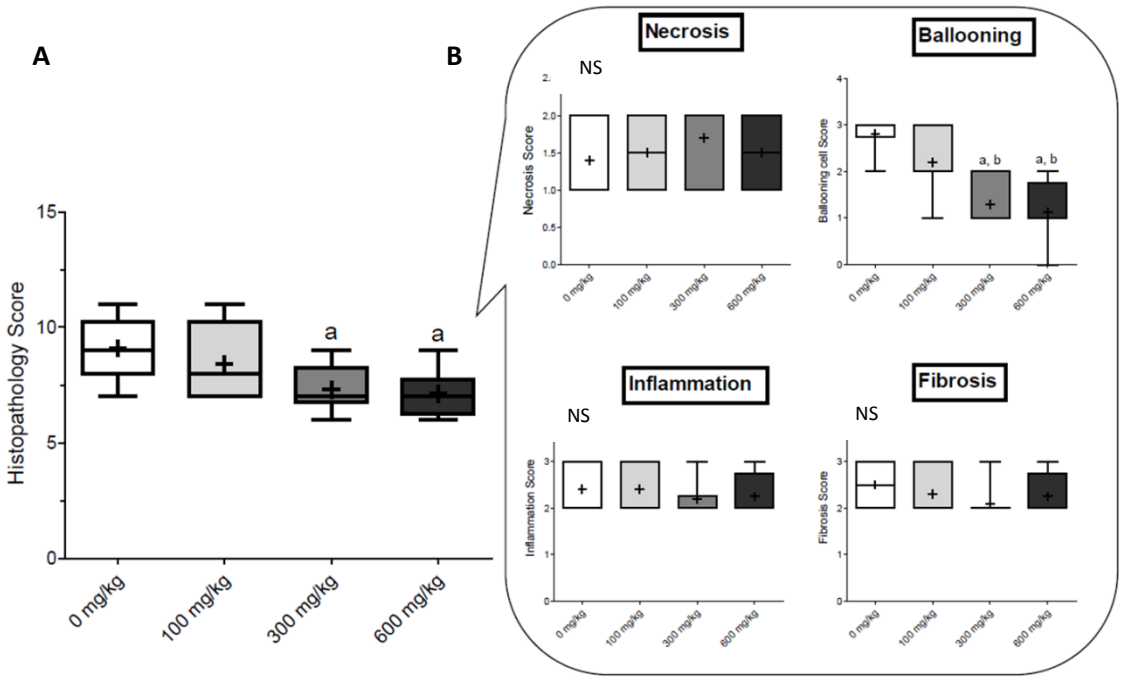

To evaluate the intensity of fibrosis in liver, a Sirius Red staining of liver tissue slides has been performed, and average Sirius Red-positive area of four representative images of each liver sample was calculated using image processing program ImageJ **(Figure 10)**. There was a significant decrease in Sirius Red-positive area percentage in CCl_4+300 mg/kg pirfenidone diet group compared to CCl_4+CD group, and similarly significant decrease compared to both CCl_4+CD and CCl_4+100 mg/kg pirfenidone diet groups. There was no significant difference in Sirius Red-positive area percentage between CCl_4+300 mg/kg pirfenidone diet and CCl_4+600 mg/kg pirfenidone diet groups.

Figure 10. Representative images of Sirius Red staining of liver (A, B) and Sirius Red-positive area quantification (C) in dose-finding study (PFD_DS). All data are presented as mean ± SD. [a]$p < 0.05$, compared to CCl_4+CD group; [b]$p < 0.05$, compared to CCl_4+PFD (100mg/kg) group. Original magnification is x100

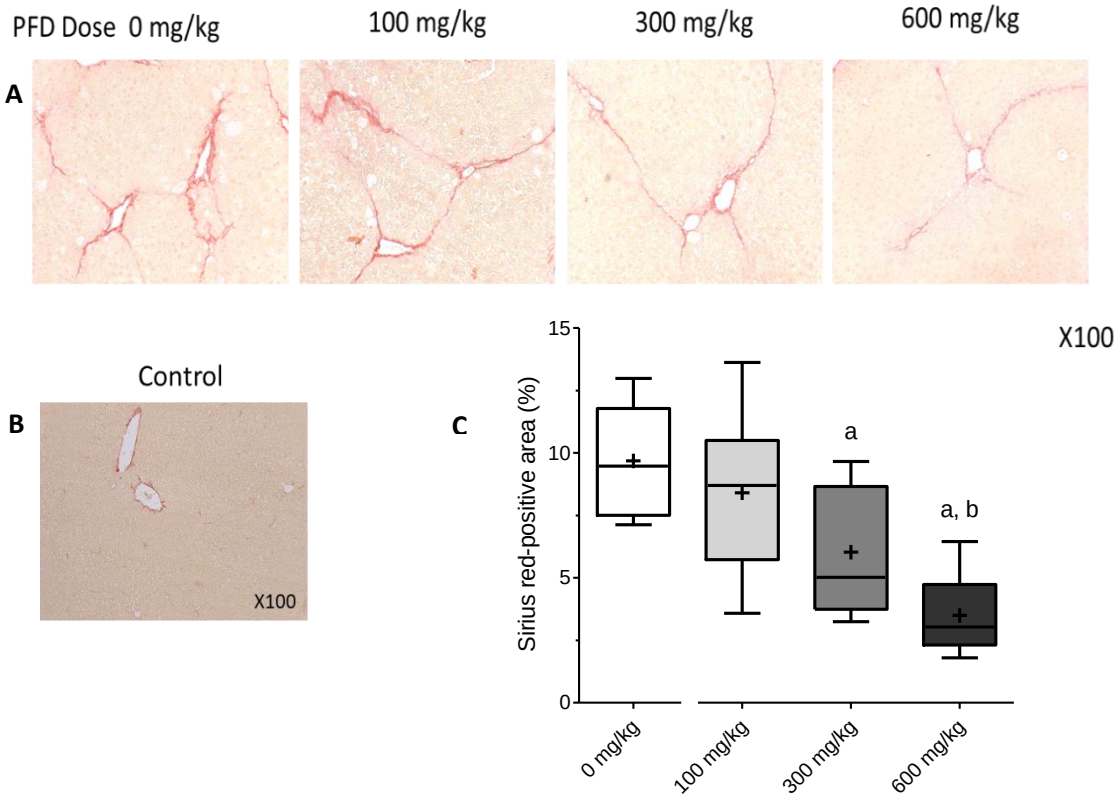

Immunohistochemistry

Immunohistochemical staining by anti-CD68 antibody was performed, and the manual quantification of CD68-positive cells of four representative images of each liver sample showed no significant difference among treatment groups **(Figure 11)**.

Figure 11. Representative images of CD68 staining of liver (A, B) and CD68-positive cells count (C) in dose-finding study (PFD_DS). All data are presented as mean ± SD. NS describes no significant difference among groups. Original magnification is x200

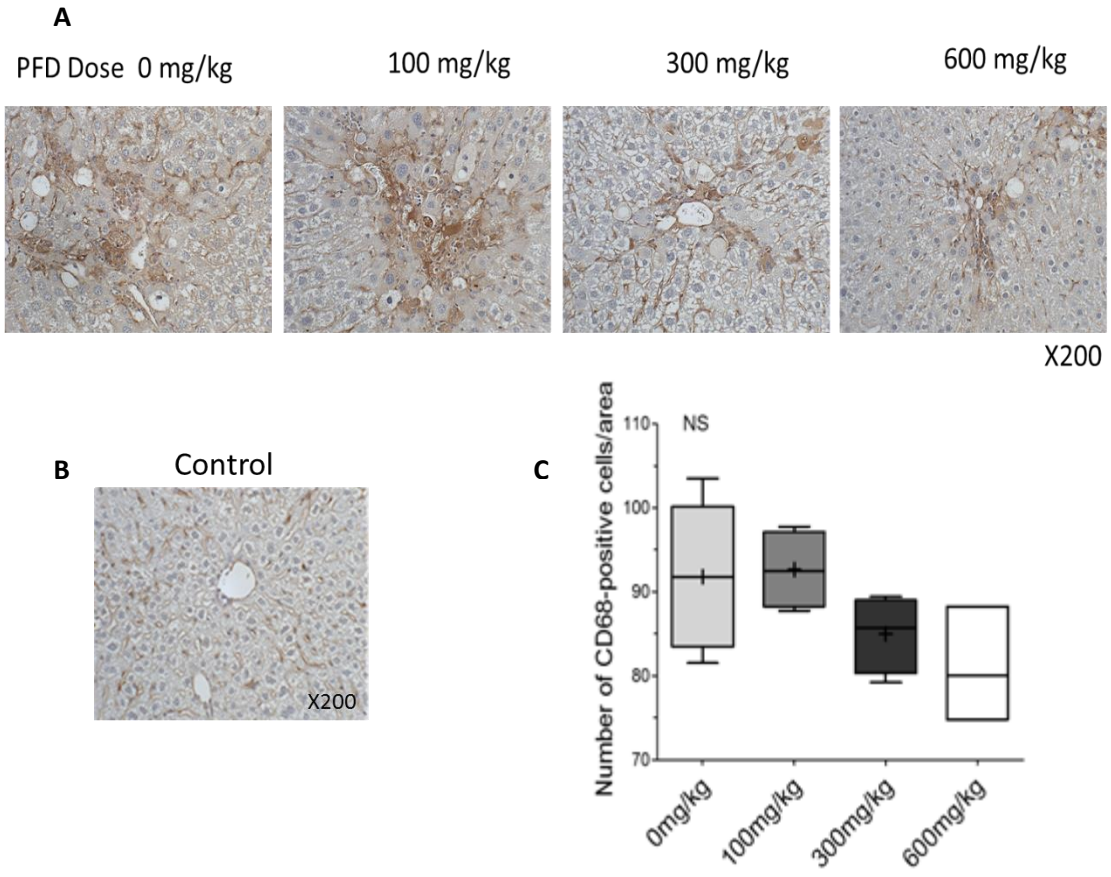

KIM-1 staining of kidney tissue was performed to help identify the extent of possible kidney injury. Manual quantification of KIM-1 positive tubules was conducted, and subsequent analysis showed no significant difference in number of KIM-1 positive tubules among treatment groups **(Figure 12, Panels A, B, C).** There was no significant difference in gene expression of hepatitis A virus cellular receptor 1 (*Kim1*) among groups **(Figure 12, Panel D).**

Figure 12. Representative images of KIM-1 staining of kidney (A, B), KIM-1-positive tubules count (C), and kidney *Kim1* mRNA expression (D) in dose-finding study (PFD_DS). All data are presented as mean ± SD. NS describes no significant difference among groups. Original magnification is x200

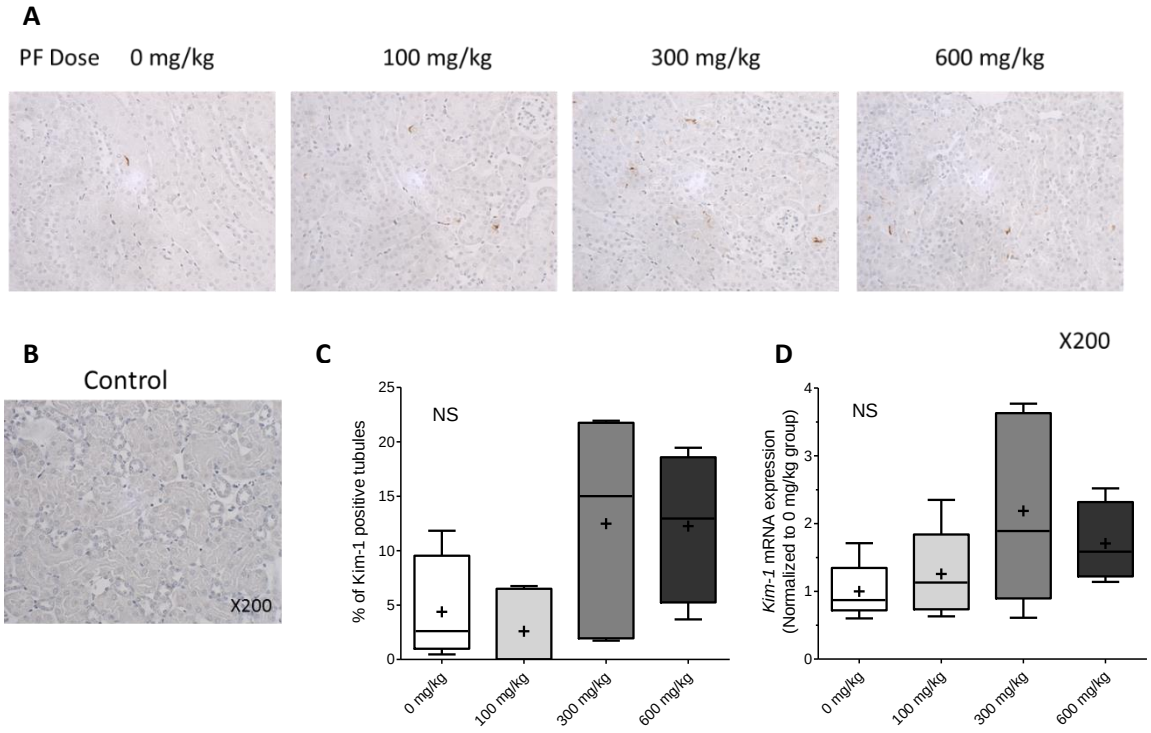

Gene expression of profibrogenic proteins in liver and gene expression of CYP450 family proteins in kidney

To assess expression of certain genes in liver and kidney, RNA isolation with subsequent quantitative reverse transcription polymerase chain reaction was performed.

In liver, there was no significant inter-group difference in gene expression of assessed profibrogenic protein markers, specifically *Timp1*, *Nqo1*, *Epcam*, *Cd68*, *Afp*, and *Krt7*. (data not shown).

In both liver and kidney, there was no significant inter-group difference in gene expression of proteins of cytochrome P450 enzyme family, specifically *Cyp1a2*, *Cyp2b10*, *Cyp2e1*, *Cyp3a11*, and *Cyp4a10*. (data not shown).

Western blot analysis of CYP2E1

To assess CYP2E1 protein levels in liver, Western blot technique was conducted, and its results showed significant increase in CYP2E1 protein levels in livers of mice in CCl_4+300 mg/kg pirfenidone diet treatment group, as compared to CCl_4+CD group **(Figure 13)**.

Figure 13. CYP2E1 protein levels in liver in dose-finding study (PFD_DS). Data is presented as mean ± SD. $^{a}p < 0.05$, compared to CCl_4+CD group (A). Detected CYP2E1 and β-actin protein bands across treatment groups are shown on (B). Representative image of Amido Black stain of proteins on membrane is shown on (C).

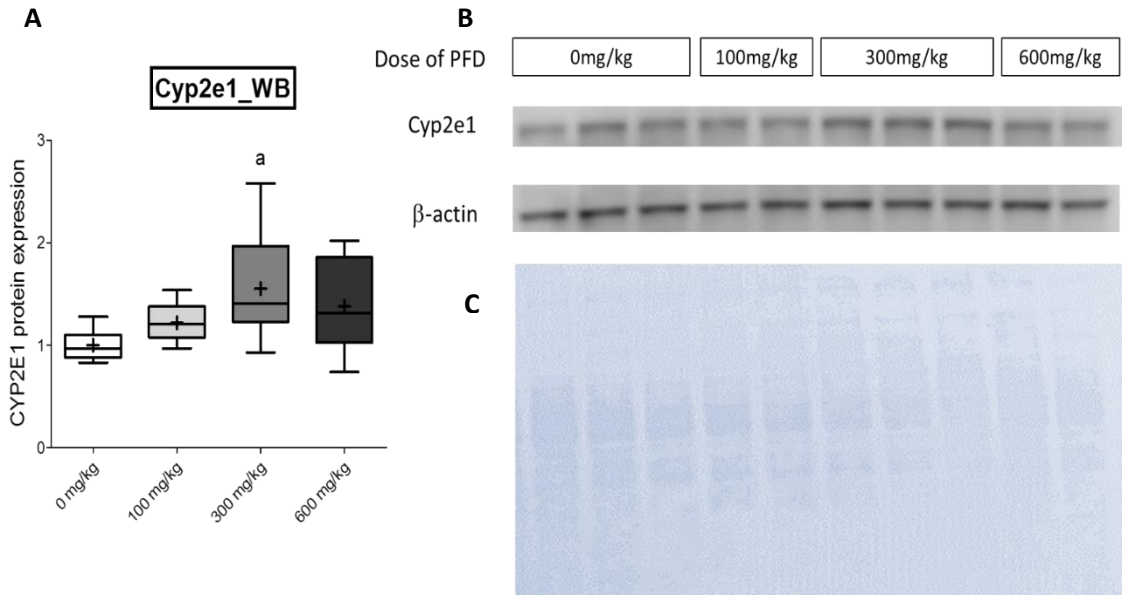

Results of sub-chronic study (PFD_AS)

PFD_AS is a 14-week subchronic study, in which 20 male B6C3F1/J mice were treated with CCl_4 (0.2 ml/kg intraperitoneal injections twice a week), while being on 300 mg/kg pirfenidone diet. Experimental design for this study is presented in **Figure 3.**

Body and organ weight

Body weight was assessed regularly to track the general state of health of animals. Animals in every group were gaining body weight over the duration of the study; mice in CD+CCl_4 and PFD+CCl_4 groups were gaining weight slower as compared to CD+OO and PFD+OO groups **(Figure 14).**

Figure 14. Body weight change in sub-chronic study (PFD_AS) among treatment groups

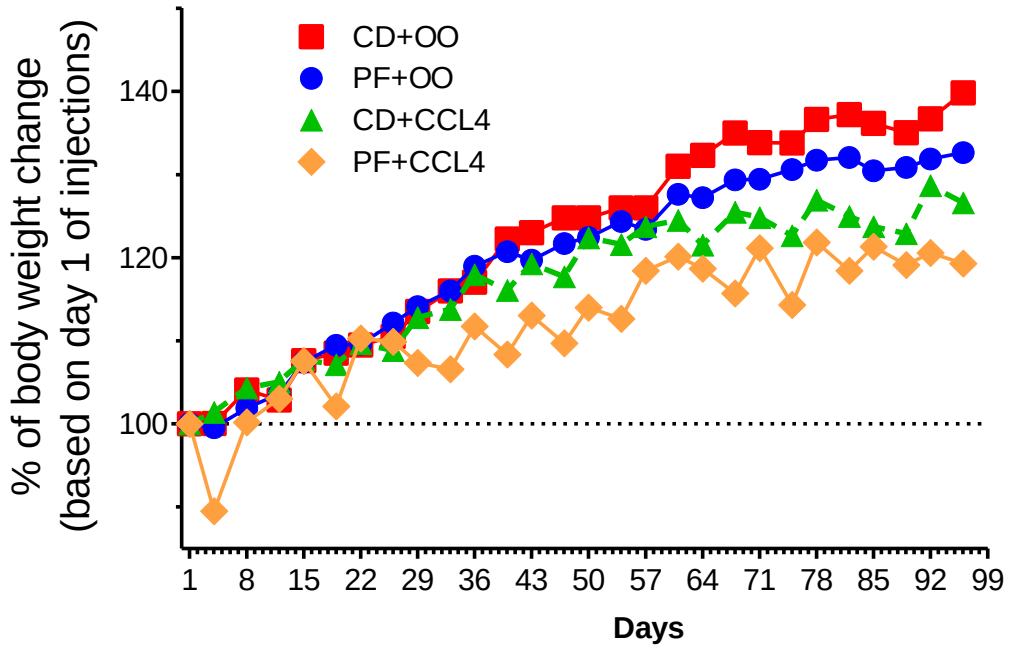

A noticeable 10% drop in body weight was observed in PFD+CCl_4 group, which may be explained by change in eating habits after the initiating intraperitoneal injections and a new diet; after adjustment to procedure and change in diet, their weight started to increase after day 4 of injections. In addition, minor fluctuations in body weight among all treatment groups were observed throughout the study.

Liver-to-body weight ratio was significantly increased in OO+PFD, CCl_4+CD, and CCl_4+PFD groups, compared to CCl_4+CD group **(Figure 15).**

There was no significant difference in kidney-to-body weight ratio among the treatment groups **(Figure 15).**

Spleen-to-body weight ratio was significantly higher in CCl_4+CD and CCl_4+PFD groups in comparison to both OO+CD and OO+PFD groups **(Figure 15).**

Figure 15. Organ-to-body weight ratios in sub-chronic study (PFD_AS). All data are presented as mean ± SD. $^{a}p < 0.05$, compared to OO+CD group; $^{b}p < 0.05$, compared to OO+PFD group; NS describes no significant difference among groups

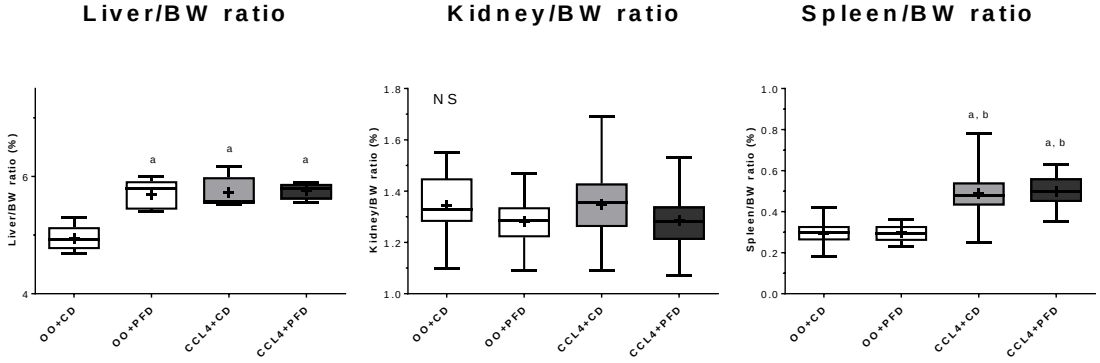

Serum clinical chemistry

Alanine aminotransferase (ALT) serum level was significantly increased in CCl_4+PFD treatment group **(Figure 16).**

Figure 16. Serum ALT in sub-chronic study (PFD_AS). All data are presented as mean ± SD. [a]$p < 0.05$, compared to OO+CD group; [b]$p < 0.05$, compared to OO+PFD group

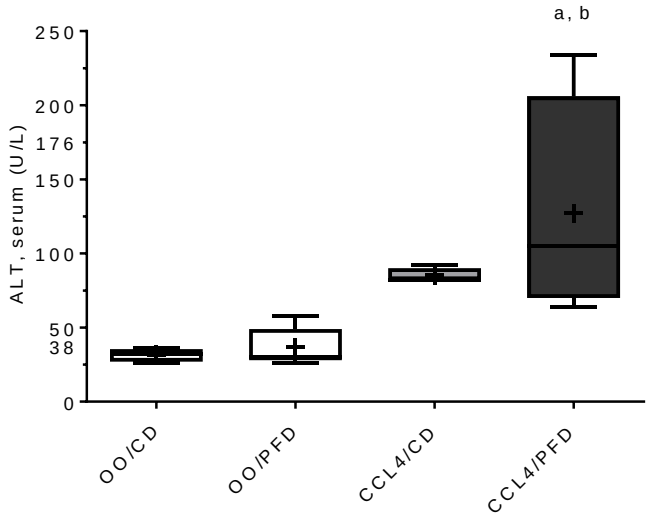

Histopathological evaluation of liver tissue

Hematoxylin and eosin staining of liver tissue slides was performed. In the centrilobular region, cellular infiltration (inflammation) and fibrosis (arrow) were observed in the CCl_4+CD and CCl_4+PFD groups. Hepatocellular degeneration, necrosis, cellular infiltration (inflammation), increase in mitotic figures of hepatocytes, and fibrosis were equally observed in CCl_4+CD and CCl_4+PFD-treated mice with no significant difference between treatment groups. Total histopathology score was calculated, using established parameters of *necrosis, ballooning, inflammation,* and *fibrosis* **(Figure 17).** Both CCl_4+CD and CCl_4+PFD treatment groups have shown similar histopathology score values with no significant difference between them. Representative image of H&E staining of mouse liver from CCl_4+CD treatment group is shown in **Figure 18**.

Figure 17. Total histopathology score in sub-chronic study (PFD_AS). All data are presented as mean ± SD. NS describes no significant difference among groups

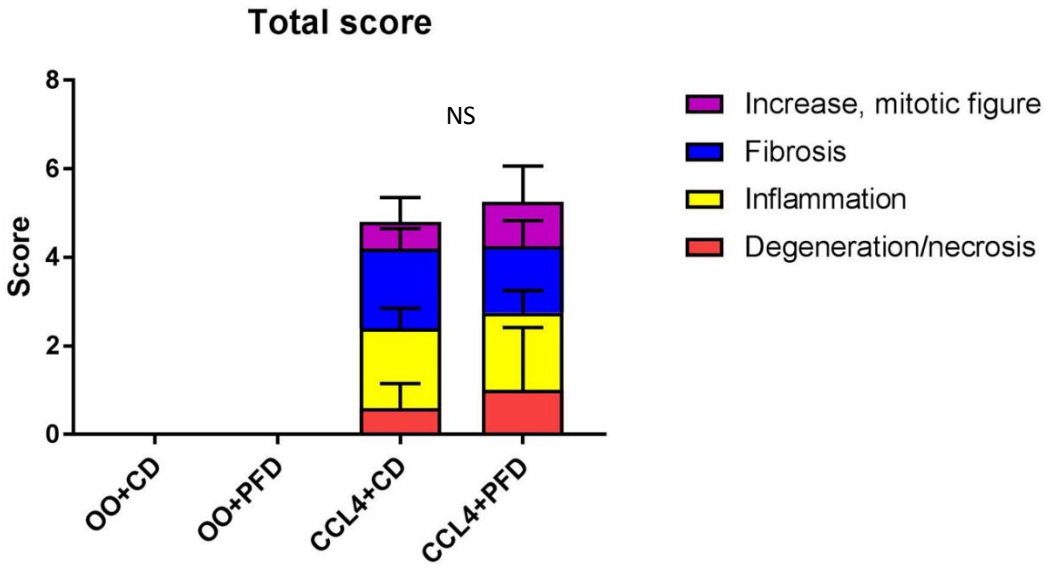

Figure 18. Representative images of CCl_4-treated, H&E stained mouse liver with administration of different diets in sub-chronic study (PFD_AS). Cellular infiltration and fibrosis are shown by *arrow*. Original magnification is x200

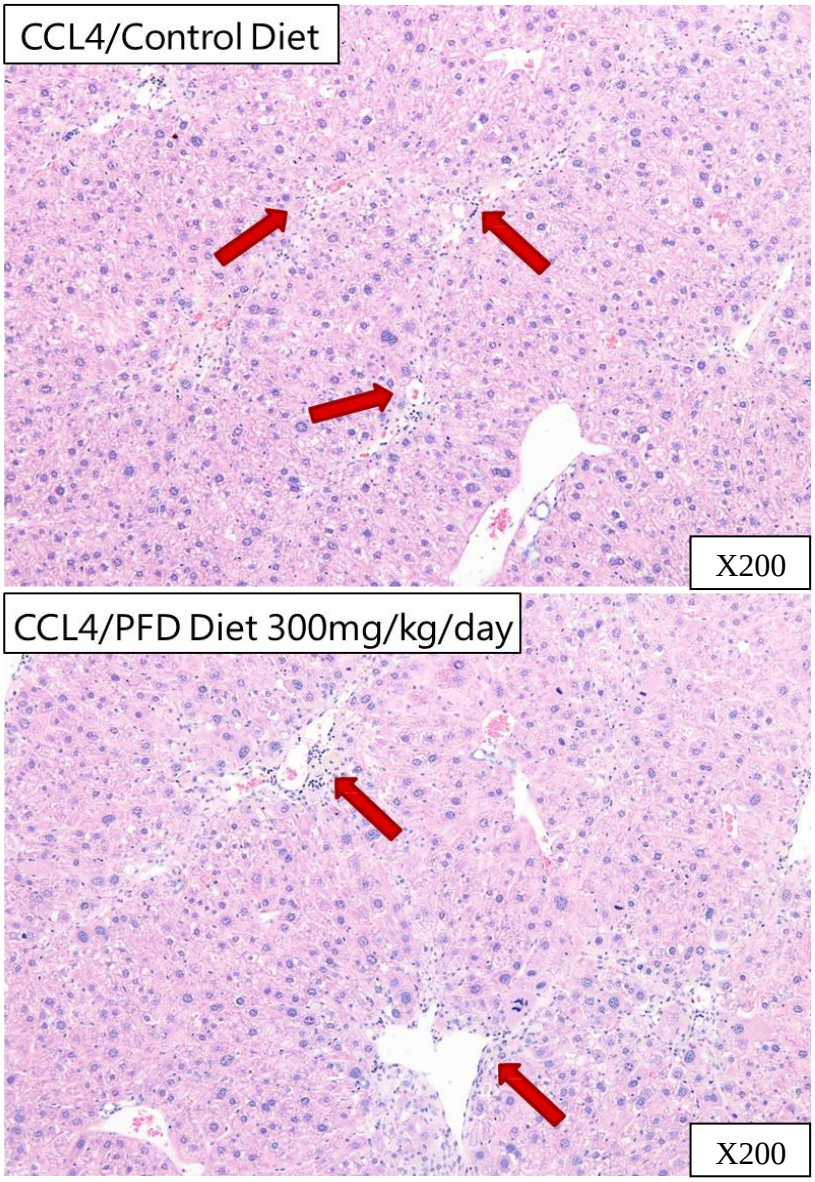

Sirius Red staining of liver tissue slides showed a significant reduction in Sirius Red-positive area percentage in CCl_4+PFD group compared to CCl_4+CD group **(Figure 19).**

Figure 19. Representative images of Sirius Red staining of liver (A) and Sirius Red-positive area quantification (B) in sub-chronic study (PFD_AS). Data is presented as mean ± SD. [a]$p < 0.05$, compared to OO+CD group; [b]$p < 0.05$, compared to OO+PFD group; [c]$p < 0.05$, compared to CCl_4+CD group. Original magnification is x100

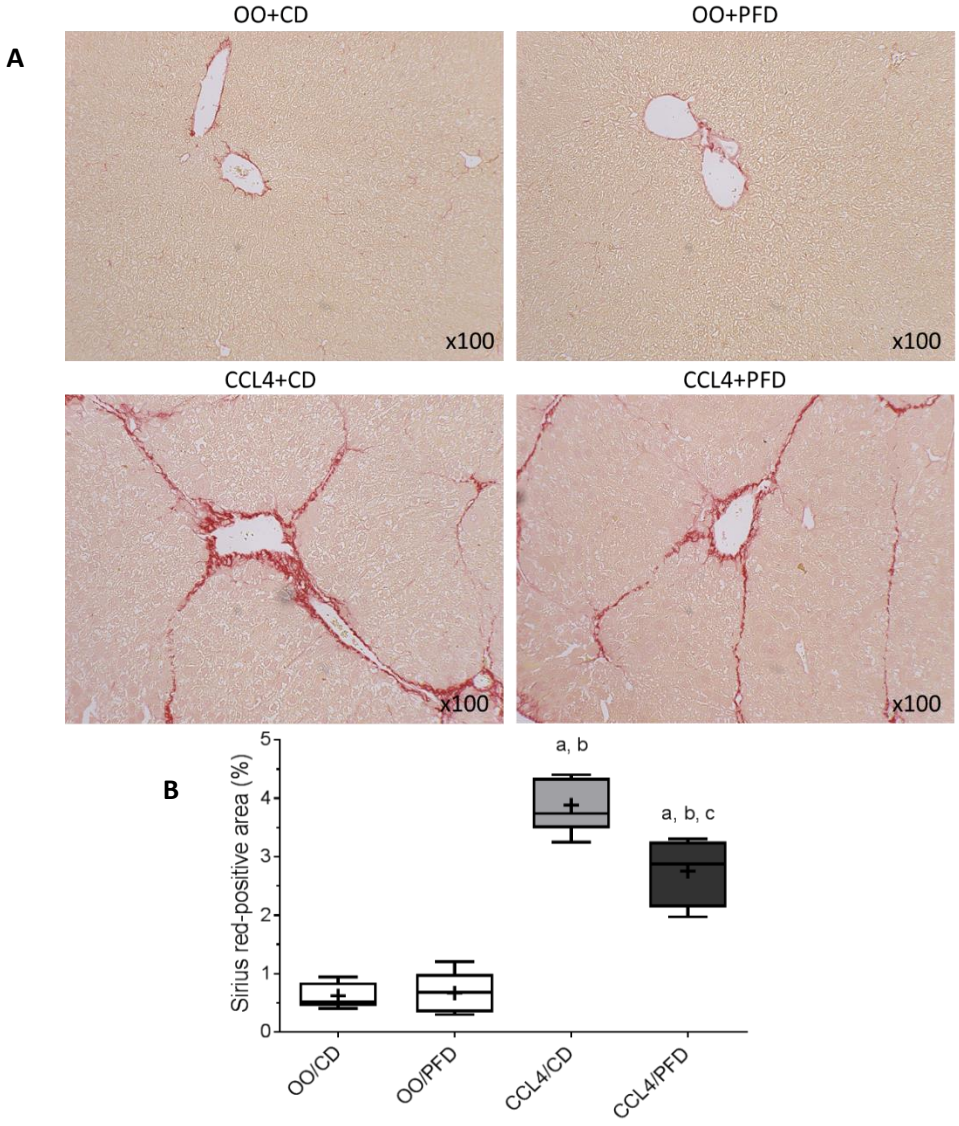

Immunohistochemistry

There was no significant difference in number of KIM-1 positive tubules and in *Kim1* gene expression among treatment groups **(Figure 20).**

Figure 20. Representative images of KIM-1 staining of kidney (A), KIM-1-positive tubules count (B), and kidney *Kim1* mRNA expression (C) in sub-chronic study (PFD_AS). Scatter plot for % of KIM-1 positive tubules is shown (line, median; whiskers, standard deviation). KIM-1 mRNA expression data is presented as mean ± SD. NS - no significant difference. Original magnification is x200

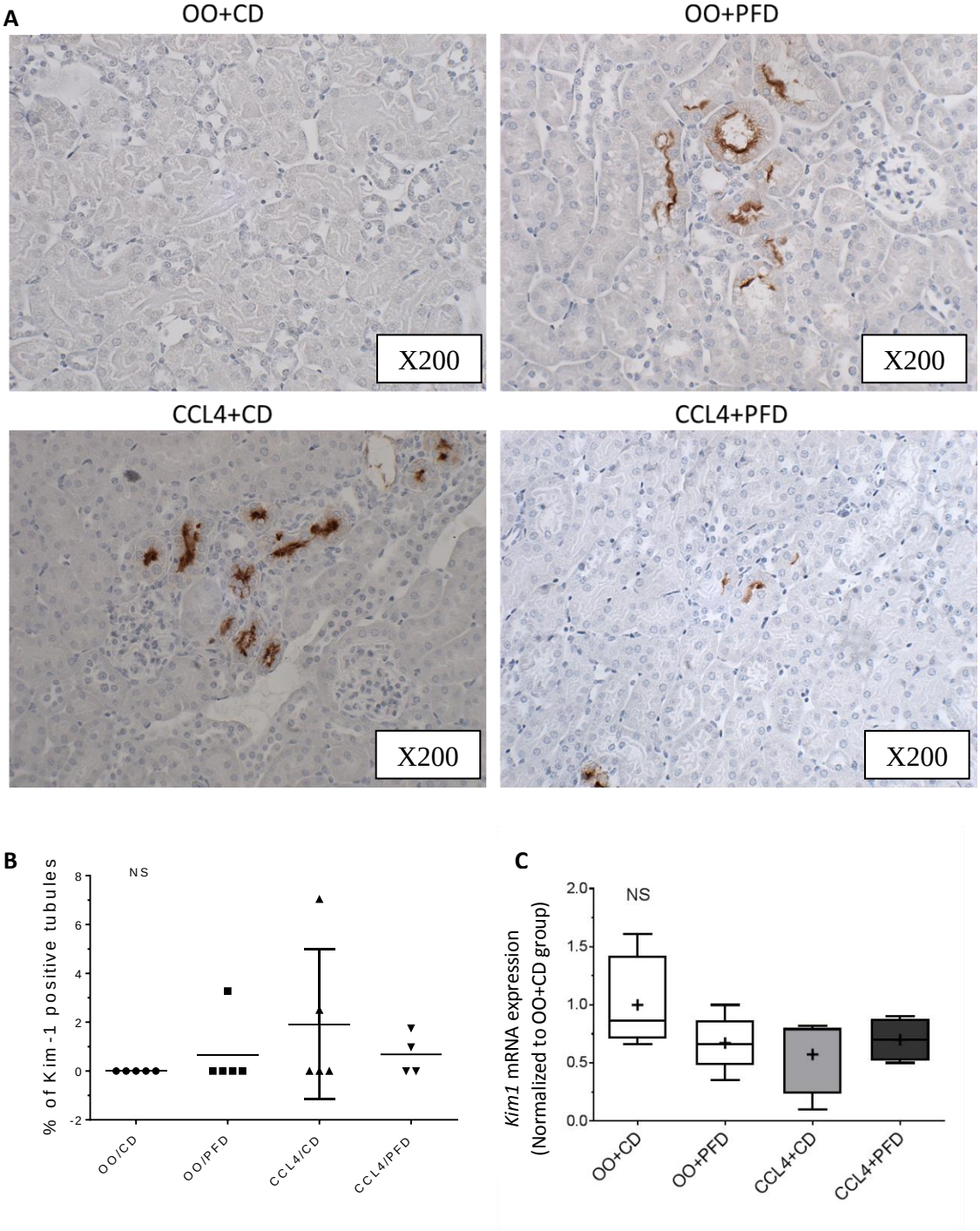

Gene expression of profibrogenic proteins in liver

To measure expression of certain genes in liver, RNA isolation with subsequent quantitative reverse transcription polymerase chain reaction was conducted.

In both treatment groups receiving CCl_4, there was a significant increase in gene expression of several profibrogenic and proinflammatory markers, specifically of genes *Tnf, Ccr5, Nqo1,* and *Hmox1* **(Figure 21).**

Gene expression *of I11* and *Tgfb1* was significantly decreased in CCl_4+CD group **(Figure 21).**

There was no significant inter-group difference in gene expression of *Timp1* **(Figure 21).**

Figure 21. *Tnf (*A)*, Timp1* (B)*, Il1* (C)*, Tgfb1* (D)*, Ccr5* (E)*, Nqo1* (F)*,* and *Hmox1* (G) mRNA expression in liver in sub-chronic study (PFD_AS). All data are presented as mean ± SD. [a]$p < 0.05$, compared to OO+CD group; [b]$p < 0.05$, compared to OO+PFD group; [c]$p < 0.05$, compared to CCl_4+CD group

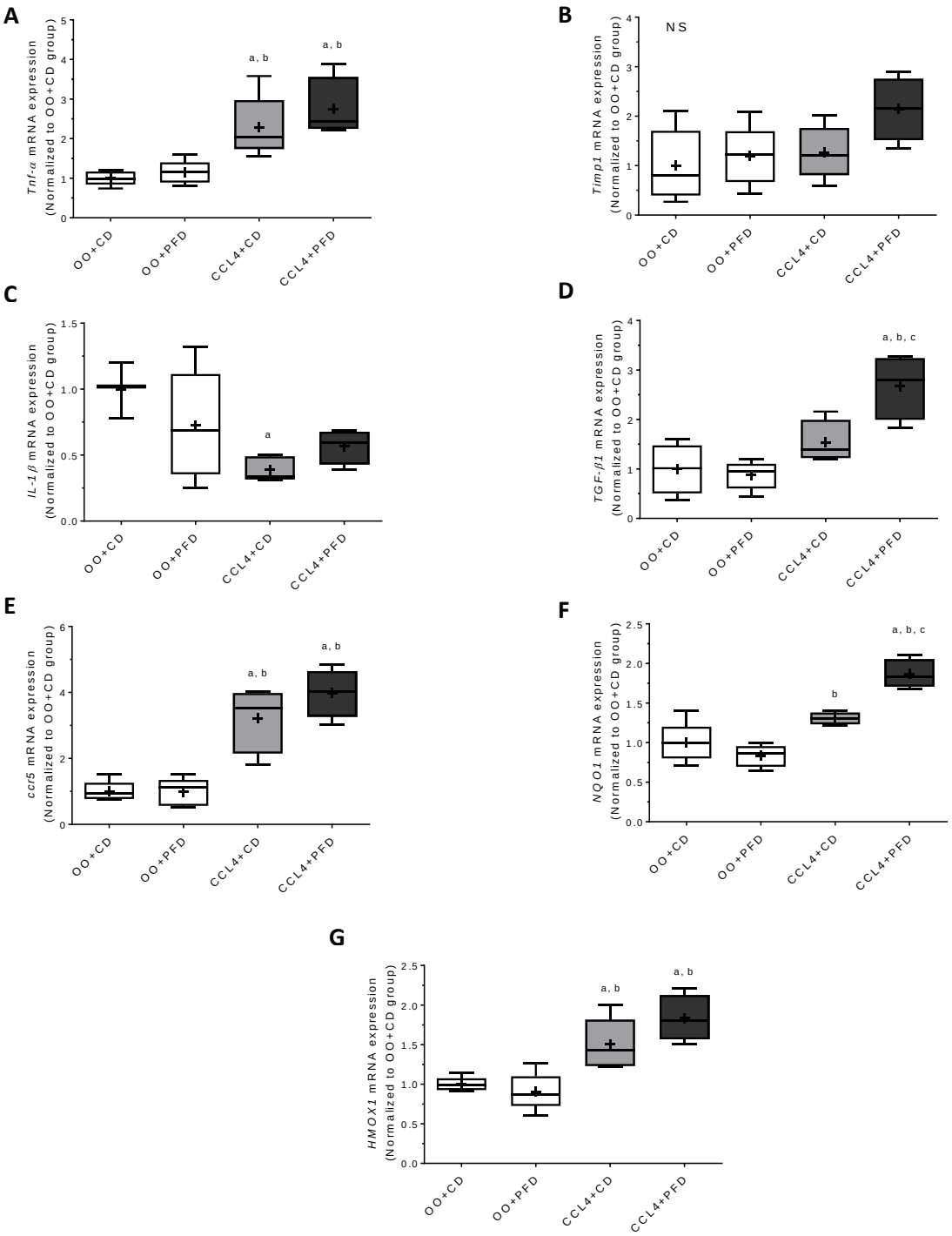

Results of anti-cancer study (PFD_MS)

PFD_MS is a 24-week anti-cancer study, in which 112 male B6C3F1/J mice were exposed to single injection of either N-nitrosodiethylamine (DEN) or phosphate-buffered saline, followed with 14-week treatment by olive oil or CCl_4 in combination with pirfenidone (300 mg/kg) or control diet. Experimental design for this study is shown in **Figure 4.**

Body and organ weight

Animals in every group were gaining body weight over the duration of the study; mice in DEN+CD/CCl_4 and DEN+PFD/CCl_4 groups were experiencing delayed and more gradual increase in body weight in comparison to PBS+PFD/OO and DEN+PFD/OO groups **(Figure 22).**

Figure 22. Body weight change in anti-cancer study (PFD_MS) among treatment groups

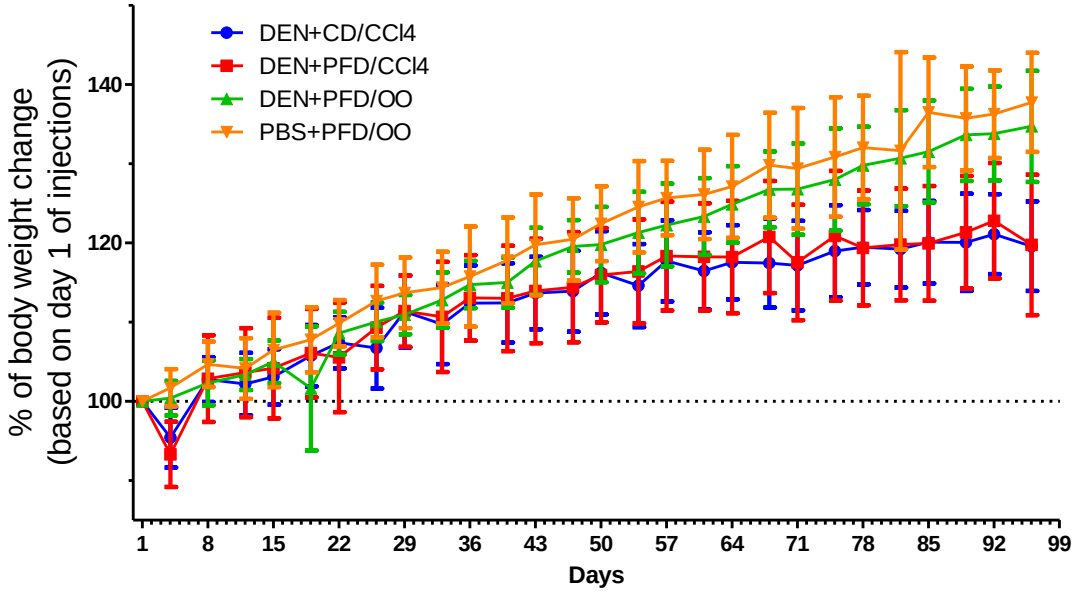

Liver-to-body weight ratio was significantly higher in DEN+CCl_4/CD and DEN+CCl_4/PFD groups, compared to PBS+OO/PFD and DEN+OO/PFD groups **(Figure 23).**

There was no significant difference in kidney-to-body weight ratio among the treatment groups **(Figure 23).**

Similarly to liver-to-body weight ratio, spleen-to-body weight ratio was significantly increased in DEN+CCl_4/CD and DEN+CCl_4/PFD groups in comparison to PBS+OO/PFD and DEN+OO/PFD groups **(Figure 23).**

Figure 23. Organ-to-body weight ratios in anti-cancer study (PFD_MS). All data are presented as mean ± SD. [a]$p < 0.05$, compared to PBS+OO/PFD group; [b]$p < 0.05$, compared to DEN+OO/PFD group. NS describes no significant difference among groups

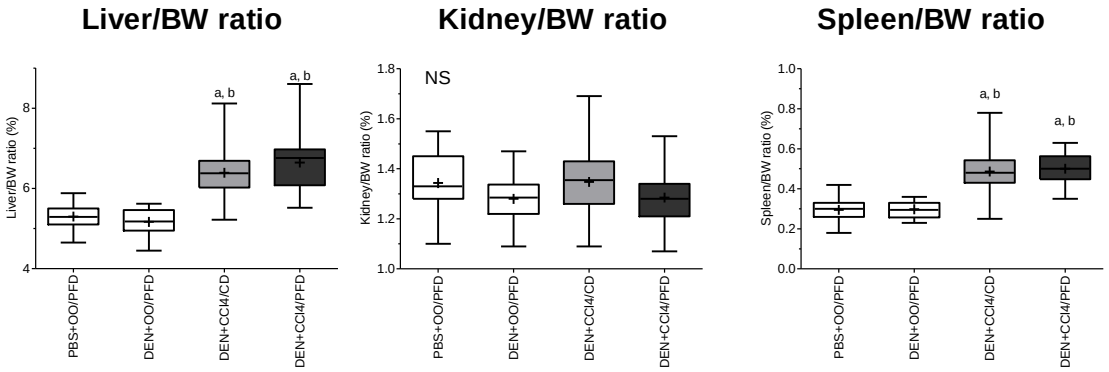

Assessment of tumor incidence, multiplicity, and size

Quantification of visible liver tissue tumors and consequent comparison of tumor amount per liver between groups did not show significant difference between pirfenidone diet and control diet groups **(Figure 24).**

Figure 24. Tumor incidence, multiplicity and size in anti-cancer study (PFD_MS). All data are presented as mean ± SD. [a]p < 0.05, compared to PBS+OO/PFD group; [b]p < 0.05, compared to DEN+OO/PFD group. NS - no significant difference

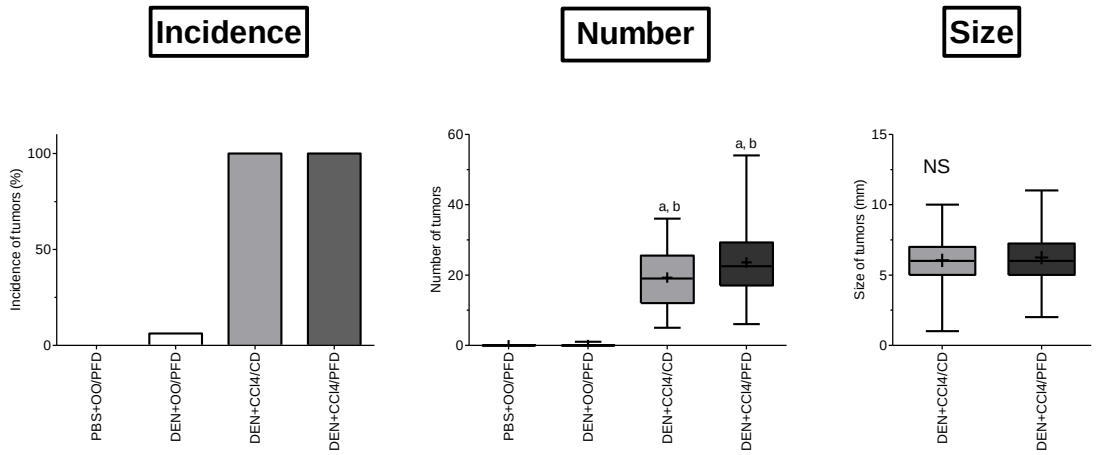

Histopathological evaluation of liver tissue

Hematoxylin and eosin staining of liver tissue slides was performed. In the DEN+CCl_4/CD, the number of tumors and foci on the section was about 1 to 10. The size of tumors in the DEN+CCl_4/CD was larger than that in the DEN+OO/PFD. All tumors were hepatocellular adenoma (benign), and all foci were of basophilic type. Representative image of H&E staining of mouse liver from DEN+CCl_4/CD treatment group is shown in **Figure 25**. In the DEN+OO/PFD group, the number of tumors and foci on the section was about 1 or 2, and all tumors were hepatocellular adenomas (benign). All foci were of basophilic type. Representative image of H&E staining of mouse liver from DEN+OO/PFD treatment group is shown in **Figure 26**.

Figure 25. Representative images of DEN/CCl_4+CD-treated, H&E-stained mouse liver in anti-cancer study (PFD_MS). Representation of hepatocellular adenomas in liver tissue is shown on (A) (original magnification x4). Closer view of hepatocellular adenoma is shown on (B) (original magnification x100)

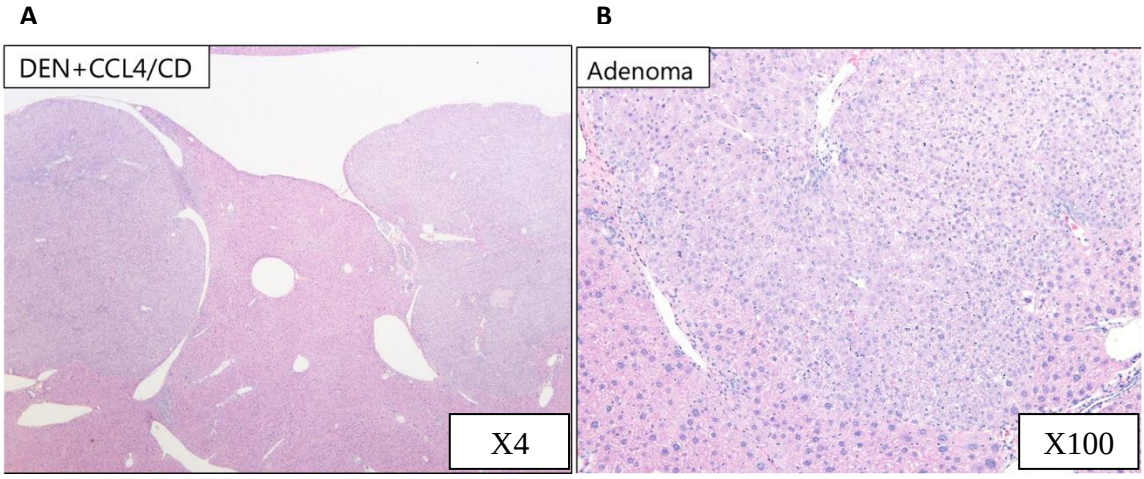

Figure 26. Representative images of DEN/OO+PFD-treated, H&E-stained mouse liver in anti-cancer study (PFD_MS). Representation of hepatocellular adenomas in liver tissue is shown on (A) (original magnification x4). Closer views of hepatocellular adenoma (B) and focus of cellular alteration (C) are represented with original magnification x100

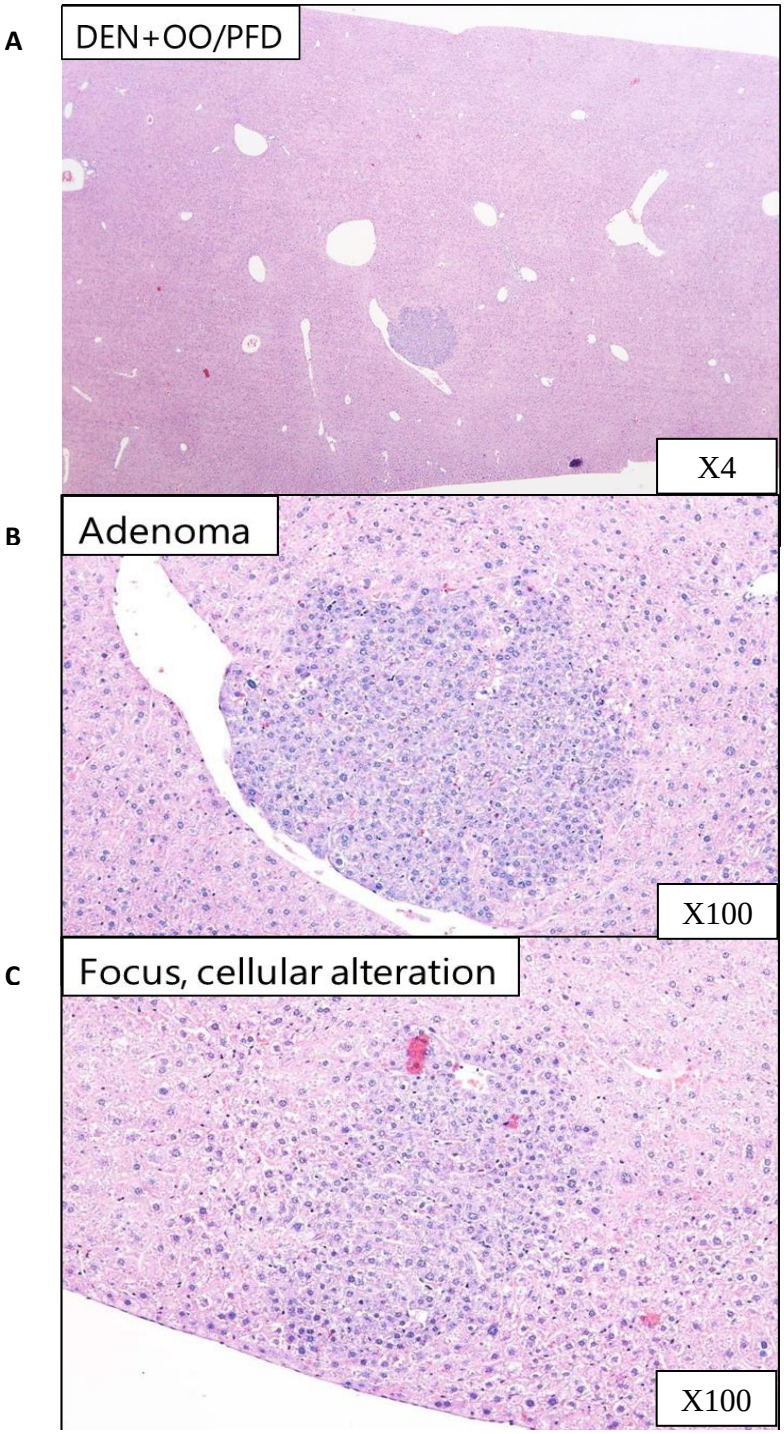

In DEN+CCl_4/PFD group, the number, size, and histopathological features of induced-tumor were of the same level as in DEN+CCl_4/CD group. Representative image of H&E staining of mouse liver from DEN+CCl_4/PFD treatment group is shown in **Figure 27**.

Figure 27. Representative images of DEN/CCl_4+PFD-treated, H&E-stained mouse liver in anti-cancer study (PFD_MS). Representation of hepatocellular adenomas in liver tissue is shown on (A) (original magnification x4). Closer view of hepatocellular adenoma is shown on (B) (original magnification x100)

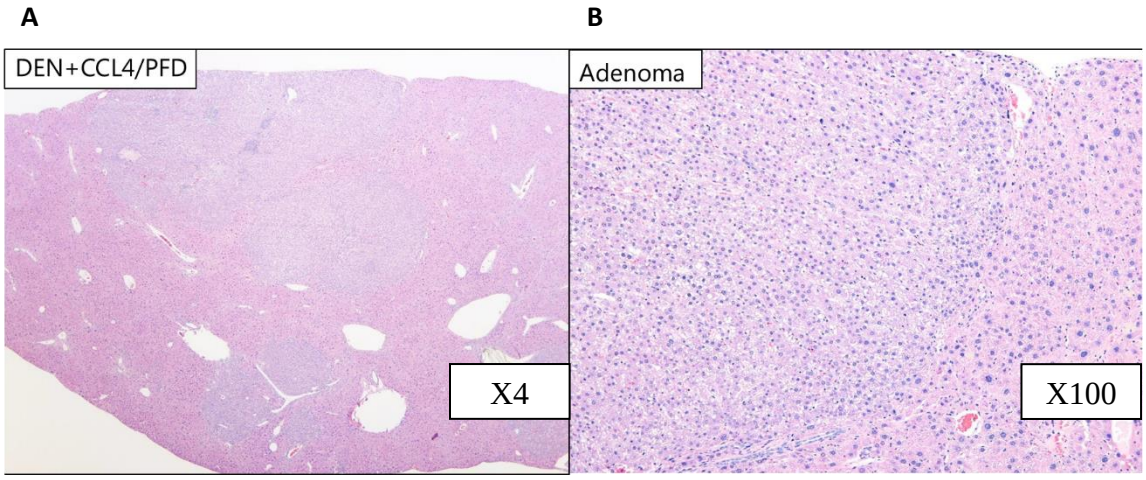

Total histopathology score was established, using the same parameters as in previous two studies. Values were similar to sub-chronic study, and there was no significant difference between DEN+CCl_4/CD and DEN+CCl_4/PFD treatment groups (data not shown).

CHAPTER V

SUMMARY, DISCUSSION, AND FUTURE DIRECTIONS

Summary

In *pirfenidone dose-finding study*, the results of Sirius Red staining showed significant reduction of collagen deposition in liver with pirfenidone administration in the event of sub-acute CCl_4-induced cytotoxic fibrosis. Decrease in the amount of "ballooning" hepatocytes was observed at 300 and 600 mg/kg doses. Decrease in serum transaminase levels supported the theory of proposed beneficial effects of pirfenidone in reducing hepatocyte damage. As confirmed by results of KIM-1 staining, there was no difference in the extent of kidney injury with addition of pirfenidone compound in diet. Based on these results, it has been concluded that pirfenidone dose of 300 mg/kg/day is the lowest effective dose that shows significant reduction in the intensity of liver fibrosis, and does not cause kidney injury in in sub-acute liver fibrosis model.

In *pirfenidone sub-chronic study*, a previously established dose of 300 mg/kg has been used to examine effects of pirfenidone in 14-week treatment by CCl_4. 14-week pirfenidone treatment also decreased collagen deposition in liver. Pirfenidone administration had little effect on the markers of inflammation and liver injury. KIM-1 staining [20] showed no difference in severity of kidney injury between control diet and pirfenidone diet, which was consistent with results of dose-finding study.

In *pirfenidone anti-cancer study*, it was expected that the incidence of liver tumors induced by consecutive administration of DEN and CCl_4 will be 100%, consistent with original

model [18]. The results of tumor quantification confirmed this expectation. Addition of pirfenidone treatment did not affect incidence, multiplicity, and size of liver tumors.

Discussion

Liver fibrosis and its complications in form of liver cirrhosis and hepatocellular carcinoma constitute a major portion of morbidity and mortality in human population worldwide. Although multiple experimental preventative and therapeutic approaches were proposed to target progression of liver fibrosis and consequential carcinogenesis [1, 6], few to this date were found to bear a desirable effect that would result in reduction in intensity of liver fibrosis, and none decreased the incidence of post-fibrotic tumorigenesis in livers of experimental animals. In this context, a better understanding of anti-fibrotic effects of pirfenidone, established treatment approach for pulmonary fibrosis, was necessary to possibly enhance management options for similar condition in liver. Pirfenidone demonstrated anti-fibrotic effects in liver in both sub-acute and sub-chronic studies; however, anti-inflammatory properties were observed only in sub-acute study. In addition, as there are established mechanisms of fibrosis-associated promotion of liver carcinogenesis [5, 18], it was important to investigate the role of pirfenidone in liver tumor development. Unfortunately, pirfenidone has no effect on development of liver tumors in anti-cancer study.

Observations of reduction in liver fibrosis intensity confirm the first hypothesis stating that pirfenidone suppresses fibrogenesis in liver, which correlates well with findings of other studies [23, 24].

While a decrease in serum biomarkers of liver injury was observed is sub-acute study, the findings did not correspond to results of sub-chronic study, in which no such reduction was observed. This nonconformity may be explained by different period of exposure to hepatotoxic compound and decrease in efficacy of pirfenidone in such circumstances. It is worth noting that 3-week pirfenidone treatment decreased AST 3-fold and ALT 2-fold after 8 weeks of intoxication by CCl_4 in previously established rat model of experimental liver fibrosis [23], although the compound was administered by gavage in that case.

Findings of the current study do not demonstrate an existing effect of pirfenidone on accumulation of hepatic macrophages, which normally constitute largest non-parenchymal cell population in the liver, being involved in promotion of fibrosis through recruitment of pro-inflammatory immune cells, secretion of pro-inflammatory cytokines and chemokines, and resolution of fibrotic process by secreting metalloproteinases in late stages [25, 26]. Currently acquired data does not correspond to evidence of suppression of macrophage accumulation by pirfenidone in rat model of renal fibrosis [27]. Described differences in effects of pirfenidone on macrophage infiltration might base on evaluation of different target organs, distinctive animal species, as well as disparate treatment duration.

Gene expression of growth factors and proinflammatory cytokines (*Tgfb1, Tnf, Il1, Il6*), whose regulation and tissue levels were previously downregulated in pulmonary fibrosis [12, 28, 29] and liver fibrosis models [23, 24], was not affected by both sub-acute and sub-chronic exposure to pirfenidone (with the exception of *Tgfb1* gene expression, which was increased in sub-chronic study). The discrepancies between the findings of studies may be

caused by such differences, duration of pirfenidone treatment, duration of toxicant exposure, species and strains of animals used, and age of animals at the start of experiment.

While establishing the lowest effective dose of pirfenidone in sub-acute liver fibrosis model, special attention has been directed towards possible detrimental effects of the compound on kidney, and the conclusion has been made that pirfenidone does not affect the kidney even in the highest evaluated dose. These findings may contribute to future evaluations of safety of pirfenidone and decisions of the compound use in patients with pre-existing kidney diseases.

Although CYP2E1 enzyme is only partially involved in metabolism of pirfenidone (which is mainly metabolized by CYP1A2 enzyme), it is worth noting that change in pirfenidone dosage did not cause any shifts in CYP2E1 expression, which correlates with the existing data [12] and does not reflect any interactions between CCl_4 and pirfenidone that might affect efficacy of the latter. The absence of anti-inflammatory effects of the compound in sub-chronic cytotoxic study may have resulted from decreased efficacy of pirfenidone in presence of potent cytotoxic chemical. A possibility of interactions in CYP450 metabolism of pirfenidone and CCl_4 should be considered in establishing cause of discrepancies between current and previous studies, in which pirfenidone showed potent anti-inflammatory properties [23, 30].

Finally, cytotoxic liver fibrosis model might not be the best appropriate tool for evaluation of pirfenidone effects, and anti-fibrotic potential of the compound may be better evaluated in studies utilizing milder and more gradual fibrogenic treatment, such as dietary exposure

to DDC (3,5-diethoxycarbonyl-1,4-dihydrocollidine), or sub-chronic treatment with ethanol by oral gavage or implanted intragastric tubes.

The second hypothesis, which addressed possible role of pirfenidone in reduction of incidence, size, and multiplicity, was refuted.

It is worth noting that the findings regarding tumor incidence with usage of DEN and CCl_4 – induced liver cancer model were consistent with the original protocol [18]. Model chosen to evaluate pirfenidone in suppression of liver tumorigenesis might not fully reflect anti-fibrotic and, subsequently, anti-cancer properties of compound due to severity of carcinogenic effect of combined DEN and CCl_4 treatment. Assessment of pirfenidone anti-cancer efficacy may be further conducted with possibly more beneficial outcomes using different liver tumorigenesis model with lower incidence of tumors, such as with aflatoxin B1 or thioacetamide treatment [17].

Efficacy of pirfenidone might be more pronounced in the event of oral gavage treatment instead of continuous voluntary exposure to drug-containing diet [23]. Anti-fibrotic properties of pirfenidone might diminish over time in case of diet location in animal cage for several days at the time at least.

Previously conducted studies demonstrated important role of pirfenidone in inhibition of pancreatic cancer desmoplasia by regulating stellate cells *in vitro* [31] and enhancement of the efficacy of combined radiation and sunitinib therapy in Lewis lung carcinoma [32]. Current study did not exhibit positive effects of pirfenidone on tumorigenesis in liver, which may be explained by specific mechanism of action of the compound and differences

in pathogenesis of these diseases. Mouse strain variabilities and possible effects of CCl_4 on pirfenidone metabolism by CYP450 system should also be considered.

Future directions

Liver fibrosis is a major health problem in the United States and developing countries. Discovery of effective medication for prevention and treatment of liver fibrosis development will reduce incidence of the disease, broaden therapeutic choices, and improve quality of life of affected individuals.

It could be stated that pirfenidone compound has promising beneficial effects, which may find application in treatment of human hepatic fibrosis caused by a diversity of causes, and results of this study may be helpful in determining directions and strategies for future pre-clinical studies and clinical trials of pirfenidone compound.

Additionally, other experimental treatments may be applied in similar setting of cytotoxic liver fibrosis caused by CCl_4, both as individual approaches and in combination with pirfenidone administration.

Considering absence of anti-cancer effect of pirfenidone in this study, it may be worth to examine application of other experimental approaches for prevention of hepatocellular carcinoma in existing DEN and CCl_4 - induced mouse model of fibrosis and inflammation-associated hepatocellular carcinoma, such as S-Adenosylmethionine [33].

REFERENCES

1. Bataller, R. and D.A. Brenner, *Liver fibrosis.* J Clin Invest, 2005. **115**(2): p. 209-18.

2. Schuppan, D. and N.H. Afdhal, *Liver cirrhosis.* Lancet, 2008. **371**(9615): p. 838-51.

3. Wolf, D.C. *Cirrhosis*. 2017 [cited 2017 18 Feb]; Available from: http://emedicine.medscape.com/article/185856-overview.

4. Cicalese, L. *Hepatocellular carcinoma*. 2016 [cited 2017 18 Feb]; Available from: http://emedicine.medscape.com/article/197319-overview.

5. Uehara, T., G.R. Ainslie, K. Kutanzi, I.P. Pogribny, L. Muskhelishvili, et al., *Molecular mechanisms of fibrosis-associated promotion of liver carcinogenesis.* Toxicol Sci, 2013. **132**(1): p. 53-63.

6. Rosenbloom, J., F.A. Mendoza, and S.A. Jimenez, *Strategies for anti-fibrotic therapies.* Biochim Biophys Acta, 2013. **1832**(7): p. 1088-103.

7. Jo, H.E., S. Randhawa, T.J. Corte, and Y. Moodley, *Idiopathic pulmonary fibrosis and the elderly: diagnosis and management considerations.* Drugs Aging, 2016. **33**(5): p. 321-34.

8. Mulhall, A., A. Cole, and S. Patel, *Efficacy and safety of nintedanib in idiopathic pulmonary fibrosis, cytisine versus nicotine for smoking cessation, and FACED score for non-cystic fibrosis bronchiectasis.* Am J Respir Crit Care Med, 2015. **192**(2): p. 249-51.

9. Richeldi, L., R.M. du Bois, G. Raghu, A. Azuma, K.K. Brown, et al., *Efficacy and safety of nintedanib in idiopathic pulmonary fibrosis.* N Engl J Med, 2014. **370**(22): p. 2071-82.

10. Wuyts, W.A., M. Kolb, S. Stowasser, W. Stansen, J.T. Huggins, et al., *First data on efficacy and safety of nintedanib in patients with idiopathic pulmonary*

fibrosis and forced vital capacity of </=50 % of predicted value. Lung, 2016. **194**(5): p. 739-43.

11. Inomata, M., K. Kamio, A. Azuma, K. Matsuda, N. Kokuho, et al., *Pirfenidone inhibits fibrocyte accumulation in the lungs in bleomycin-induced murine pulmonary fibrosis.* Respiratory Research, 2014. **15**(1): p. 16.

12. Kim, E.S. and G.M. Keating, *Pirfenidone: a review of its use in idiopathic pulmonary fibrosis.* Drugs, 2015. **75**(2): p. 219-230.

13. Xie, Y., H. Jiang, Q. Zhang, S. Mehrotra, P.W. Abel, et al., *Upregulation of RGS2: a new mechanism for pirfenidone amelioration of pulmonary fibrosis.* Respir Res, 2016. **17**(1): p. 103.

14. Wang, F., T. Wen, X.Y. Chen, and H. Wu, *Protective effects of pirfenidone on D-galactosamine and lipopolysaccharide-induced acute hepatotoxicity in rats.* Inflamm Res, 2008. **57**(4): p. 183-8.

15. Lopez-de la Mora, D.A., C. Sanchez-Roque, M. Montoya-Buelna, S. Sanchez-Enriquez, S. Lucano-Landeros, et al., *Role and new insights of pirfenidone in fibrotic diseases.* Int J Med Sci, 2015. **12**(11): p. 840-7.

16. Hayashi, H. and T. Sakai, *Animal models for the study of liver fibrosis: new insights from knockout mouse models.* Am J Physiol Gastrointest Liver Physiol, 2011. **300**(5): p. G729-38.

17. Heindryckx, F., I. Colle, and H. Van Vlierberghe, *Experimental mouse models for hepatocellular carcinoma research.* Int J Exp Pathol, 2009. **90**(4): p. 367-86.

18. Uehara, T., I.P. Pogribny, and I. Rusyn, *The DEN and CCl4 -induced mouse model of fibrosis and inflammation-associated hepatocellular carcinoma.* Curr Protoc Pharmacol, 2014. **66**: p. 14 30 1-10.

19. Lackner, C., M. Gogg-Kamerer, K. Zatloukal, C. Stumptner, E.M. Brunt, et al., *Ballooned hepatocytes in steatohepatitis: the value of keratin immunohistochemistry for diagnosis.* J Hepatol, 2008. **48**(5): p. 821-8.

20. Kondo, C., M. Aoki, E. Yamamoto, Y. Tonomura, M. Ikeda, et al., *Predictive genomic biomarkers for drug-induced nephrotoxicity in mice.* The Journal of Toxicological Sciences, 2012. **37**(4): p. 723-737.

21. Oh, R.C. and T.R. Hustead, *Causes and evaluation of mildly elevated liver transaminase levels.* Am Fam Physician, 2011. **84**(9): p. 1003-8.

22. Schmittgen, T.D. and K.J. Livak, *Analyzing real-time PCR data by the comparative C(T) method.* Nat Protoc, 2008. **3**(6): p. 1101-8.

23. Garcia, L., I. Hernandez, A. Sandoval, A. Salazar, J. Garcia, et al., *Pirfenidone effectively reverses experimental liver fibrosis.* Journal of Hepatology, 2002. **37**(6): p. 797-805.

24. Di Sario, A., E. Bendia, G. Macarri, C. Candelaresi, S. Taffetani, et al., *The anti-fibrotic effect of pirfenidone in rat liver fibrosis is mediated by downregulation of procollagen alpha1(I), TIMP-1 and MMP-2.* Dig Liver Dis, 2004. **36**(11): p. 744-51.

25. Li, H., H. You, X. Fan, and J. Jia, *Hepatic macrophages in liver fibrosis: pathogenesis and potential therapeutic targets.* BMJ Open Gastroenterol, 2016. **3**(1): p. e000079.

26. Wynn, T.A. and K.M. Vannella, *Macrophages in tissue repair, regeneration, and fibrosis.* Immunity, 2016. **44**(3): p. 450-62.

27. Chen, J.F., H.F. Ni, M.M. Pan, H. Liu, M. Xu, et al., *Pirfenidone inhibits macrophage infiltration in 5/6 nephrectomized rats.* Am J Physiol Renal Physiol, 2013. **304**(6): p. F676-85.

28. Oku, H., T. Shimizu, T. Kawabata, M. Nagira, I. Hikita, et al., *Antifibrotic action of pirfenidone and prednisolone: different effects on pulmonary cytokines and growth factors in bleomycin-induced murine pulmonary fibrosis.* Eur J Pharmacol, 2008. **590**(1-3): p. 400-8.

29. Iyer, S.N., D.M. Hyde, and S.N. Giri, *Anti-inflammatory effect of pirfenidone in the bleomycin-hamster model of lung inflammation.* Inflammation, 2000. **24**(5): p. 477-91.

30. Tsuchiya, H., M. Kaibori, H. Yanagida, N. Yokoigawa, A.H. Kwon, et al., *Pirfenidone prevents endotoxin-induced liver injury after partial hepatectomy in rats.* Journal of Hepatology, 2004. **40**(1): p. 94-101.

31. Kozono, S., K. Ohuchida, D. Eguchi, N. Ikenaga, K. Fujiwara, et al., *Pirfenidone inhibits pancreatic cancer desmoplasia by regulating stellate cells.* Cancer Res, 2013. **73**(7): p. 2345-56.

32. Choi, S.H., J.K. Nam, J. Jang, H.J. Lee, and Y.J. Lee, *Pirfenidone enhances the efficacy of combined radiation and sunitinib therapy.* Biochem Biophys Res Commun, 2015. **462**(2): p. 138-43.

33. Lu, S.C., K. Ramani, X. Ou, M. Lin, V. Yu, et al., *S-adenosylmethionine in the chemoprevention and treatment of hepatocellular carcinoma in a rat model.* Hepatology, 2009. **50**(2): p. 462-71.